

Emerging Therapeutic Potential of SIRT6 Modulators

Francesco Fiorentino, Antonello Mai,* and Dante Rotili*

Cite This: *J. Med. Chem.* 2021, 64, 9732–9758

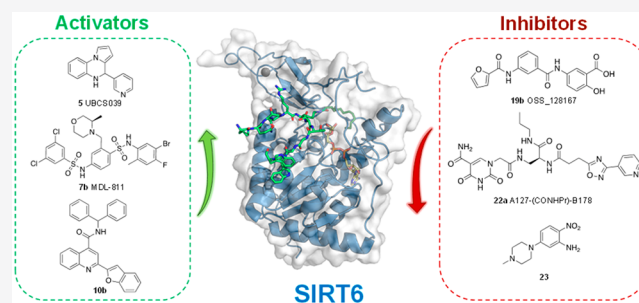
Read Online

ACCESS |

Metrics & More

Article Recommendations

ABSTRACT: Sirtuin 6 (SIRT6) is an NAD⁺-dependent protein deacetylase and mono-ADP-ribosyltransferase of the sirtuin family with a wide substrate specificity. *In vitro* and *in vivo* studies have indicated that SIRT6 overexpression or activation has beneficial effects for cellular processes such as DNA repair, metabolic regulation, and aging. On the other hand, SIRT6 has contrasting roles in cancer, acting either as a tumor suppressor or promoter in a context-specific manner. Given its central role in cellular homeostasis, SIRT6 has emerged as a promising target for the development of small-molecule activators and inhibitors possessing a therapeutic potential in diseases ranging from cancer to age-related disorders. Moreover, specific modulators allow the molecular details of SIRT6 activity to be scrutinized and further validate the enzyme as a pharmacological target. In this Perspective, we summarize the current knowledge about SIRT6 pharmacology and medicinal chemistry and describe the features of the activators and inhibitors identified so far.



■ INTRODUCTION

The sirtuin family is a class of enzymes that employs NAD⁺ as cofactor.¹ Although initially classified as class III HDACs, sirtuins (SIRT) are capable of catalyzing different reactions and possess a wide range of substrates far beyond histones.² Among them, sirtuin 6 (SIRT6) is a pivotal chromatin homeostasis modulator that deacetylates both histone and nonhistone proteins, including DNA repair factors and glucose homeostasis regulators. In addition, SIRT6 promotes the deacylation of long-chain fatty-acid groups and catalyzes the mono-ADP-ribosylation of chromatin silencing DNA repair proteins,³ including self-mono-ADP-ribosylation.⁴ Through its enzymatic activity, SIRT6 facilitates the removal of acyl groups from the ϵ -amino group of lysines and transfers ADP-ribose moieties to lysine and arginine residues of protein substrates (Figure 1).

Given the requirement of NAD⁺ for their activity, SIRTs have been regarded as pivotal proteins connecting metabolism to cellular physiology.⁵ SIRT6, being a nuclear member of this family, tightly regulates DNA repair and genome maintenance and has a pivotal role in glucose and lipid metabolism. These activities are tightly related to the central roles that SIRT6 has in aging, stem cell differentiation, and tumorigenesis.

Loss-of-function studies performed in mouse models indicated the crucial roles that SIRT6 plays for organism wellbeing. Indeed, SIRT6-deficient mice displayed alteration of glycolysis and genomic instability, ultimately leading to premature aging and shortened lifespan.^{6–8} In addition, SIRT6 deletion was associated with increased tumor aggressiveness, and later studies in human cancers identified mutations impairing SIRT6 activity.⁹ Conversely, recent studies also

described SIRT6 as a tumor promoter, hence highlighting the context-dependent role of this enzyme in cellular homeostasis.^{10,11}

Homozygous mutations leading to SIRT6 loss of activity in humans caused fetal loss associated with muscle and brain developmental deficiencies.¹² Similarly, cynomolgus monkeys bearing a SIRT6 knockout obtained through CRISPR-Cas9 suggested a primary role of SIRT6 for primates' fetal development.¹³

Conversely, SIRT6 overexpression in male mice determined an increased lifespan, and another study indicated that SIRT6 levels increase in cultured cells, mice, and rats under conditions of caloric restriction, a dietary program that protects against many aging-related changes.¹⁴

SIRT6 has been initially described as an HDAC, having histone H3 as a substrate and catalyzing the deacetylation of lysines Lys9, Lys18, and Lys56.^{15–18} Histone deacetylation is associated with compaction of chromatin and consequent transcriptional repression as well as DNA-damage response. Nevertheless, recent reports indicated that SIRT6 deacetylase catalytic activity is 100 to 1000 times lower compared to the most active SIRTs.¹⁹ In addition, the deacetylase efficiency of SIRT6 has been shown to be higher compared to deacetylation,

Received: April 1, 2021

Published: July 2, 2021



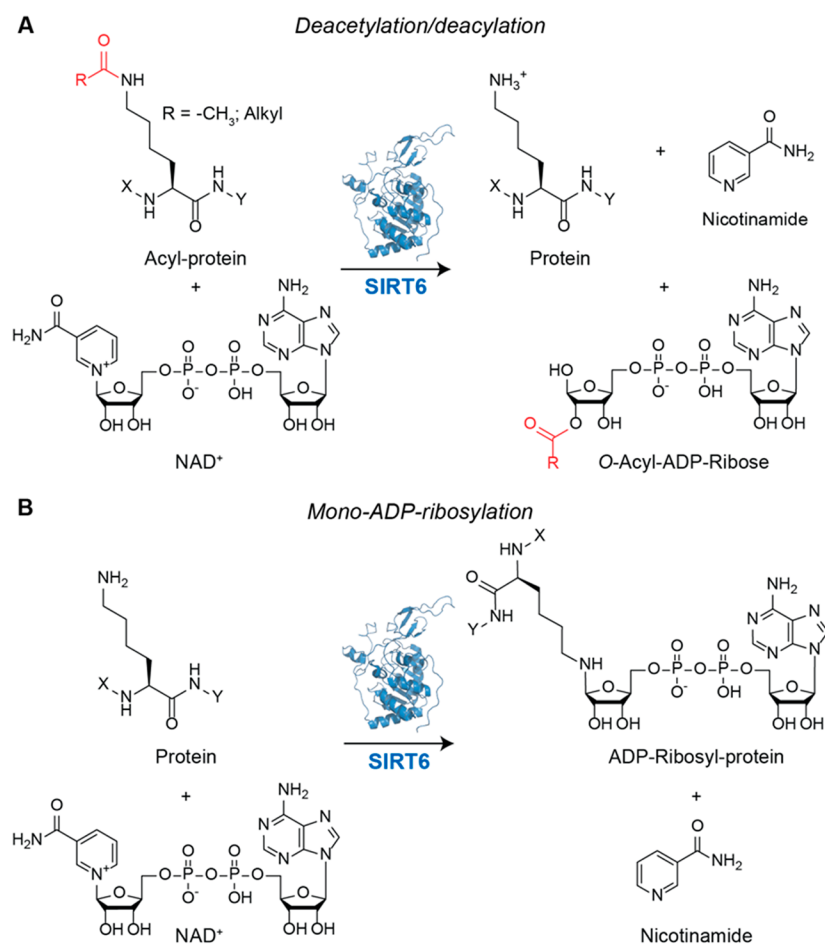


Figure 1. (A) Deacetylation/deacylation reaction catalyzed by SIRT6. The acetyl/acetyl group is transferred to an NAD⁺ acceptor, coupled with removal of nicotinamide. (B) Mono-ADP-ribosylation reaction. In this case, ADP-ribose is transferred onto the ϵ -amino group of lysine from an NAD⁺ donor. Nicotinamide and ADP-ribose protein are the products.

which can be in turn activated by small molecules, including free fatty acids (FFAs).^{20,21} For instance, *in vitro* demyristoylation activity is roughly 300 times higher than deacetylation.²² Nonetheless, the majority of studies on SIRT6 indicate deacetylation as the main reaction responsible for its cellular functions, while deacylation has only been reported in the case of TNF- α ²² and R-Ras2²³ so far. These features, along with the ability of SIRT6 to catalyze mono-ADP-ribosylation, depict a complicated picture of SIRT6 biological functions. Many details connecting the biochemical activity of SIRT6 and the observed phenotypes in both physiological and pathological conditions are still missing; hence, the main goals for future investigations consist of uncovering new SIRT6 substrates and elucidating its molecular interactors.

An important strategy for further elucidation of SIRT6 activity is played by chemical probes that through activation or inhibition of SIRT6 enzymatic activity may help to clarify the connection between SIRT6 function and the observed phenotypes. In addition, given the central role that SIRT6 plays in processes such as DNA repair, metabolism, aging, and tumorigenesis, small-molecule modulators could represent potential weapons for SIRT6-targeted treatment of diseases such as diabetes, obesity, cancer, and neurodegeneration.

■ SIRT6 STRUCTURE AND CATALYTIC MECHANISM

A key role in the investigation of SIRT6 function is played by the elucidation of its structural features. A decade has passed since the first structure of SIRT6 in complex with ADP-ribose has been solved,¹⁹ followed by the structure of SIRT6 bound to both ADP-ribose and myristoylated H3K9 peptide (Figure 2A).²² SIRT6 has two globular domains: a large Rossmann fold and a small zinc-binding region. The Rossmann fold consists of six β -sheets sandwiched between four α -helices on one side and two α -helices on the other side. This domain contains the NAD⁺ binding site as well as a hydrophobic pocket to accommodate the acyl chains of SIRT6 substrates. Differently from other SIRT6s, SIRT6 has been reported to bind NAD⁺ in the absence of the acylated substrate.¹⁹ This feature is explained by the structural differences in the NAD⁺-binding region. Indeed, SIRT6 lacks the cofactor-binding loop^{24–26} but presents a helix (α 3) that keeps its ordered structure even in the absence of the acylated peptide.¹⁹

The hydrophobic channel is shaped by residues belonging to different loops engaging hydrophobic interactions with the fatty acyl chain, as shown by Lin and colleagues (Figure 2B).²² In the presence of a myristoylated peptide, the N-terminus of SIRT6, which covers part of the hydrophobic pocket, becomes structured. The structural ordering induced by the myristoylated peptide may facilitate the catalytic process and explain the higher catalytic efficiency of long-fatty-chain deacylation compared to

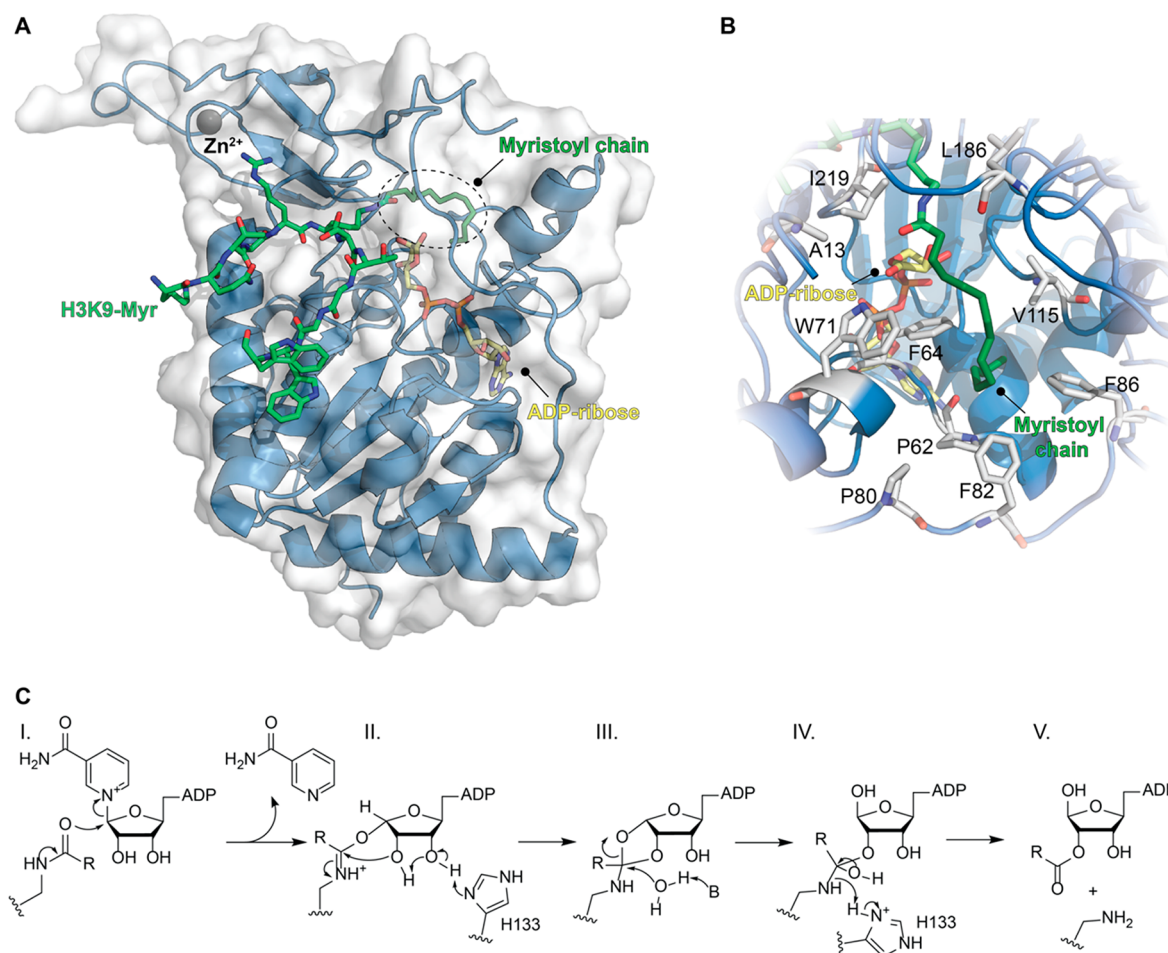


Figure 2. (A) Structure of SIRT6 in complex with H3K9-Myr (green) and ADP-ribose (yellow) bound (PDB ID: 3ZG6). (B) Focus on the hydrophobic pocket in the Rossmann fold accommodating the myristoyl chain. (C) Catalytic mechanism of SIRT6-mediated deacetylation.

deacetylation.²² It can also account for the increased deacetylation activity in the presence of FFA and small molecules. Nonetheless, there are no SIRT6 structures bound to an acetylated substrate; hence, this hypothesis is yet to be proven.

Finally, the zinc-binding motif is only structural and does not participate in the catalysis; this feature is shared by all SIRT6s and differentiates them from class I, II, and IV HDACs possessing in the active site a zinc ion essential for catalysis.²⁷

Notably, the *in vitro* deacetylase activity of SIRT6 is much lower than that of other SIRT6s, probably because of SIRT6 peculiar structural features. Nevertheless, several cell-based assays suggested that the deacetylation is the most prominent activity of SIRT6, and H3K9 was indicated as the SIRT6 main substrate.¹⁹ This is explained by the fact that SIRT6 preferably associates with histones when they are packaged in nucleosomes. Conversely, SIRT1 exhibits higher deacetylation activity toward unpacked histones. Thus, interaction with packaged histones may trigger a transition toward an active SIRT6 conformation. Hence, SIRT6 activity depends on histone packaging, thereby being lower when tested *in vitro* using free histones.²⁸ It is therefore possible that in the case of other substrates SIRT6 deacetylase activity is affected by the presence of interactors contributing to the formation of multiprotein complexes.

As mentioned above, SIRT6 deacetylase activity has been reported to be higher than deacetylation.²² However, a

functional role for SIRT6-mediated deacetylation has only been described in the case of TNF- α ²² and R-Ras2.²³ Importantly, histone deacetylation has only been indicated in preliminary *in vitro* studies. In the same study in which TNF- α deacetylation was described for the first time, Jiang et al. also showed that SIRT6 can catalyze the removal of octanoyl, myristoyl, and palmitoyl groups from H3K9 and of myristoyl from H2BK12 using synthetic histone peptides as substrates.²² A subsequent analysis was performed using a chemical biology approach, in which the SIRT6-acylated substrate was the octenoylated H3 incorporated in the nucleosome. The terminal olefin selectively could react with a tetrazine probe allowing nucleosome labeling. This study suggested that SIRT6 catalyzes the efficient deacetylation of H3K9, H3K18, and H3K27 while having low activity toward H3K4 and H3K23.²⁹ Nonetheless, the precise physiological role of histones' acylation/deacetylation equilibria need further elucidation.

The SIRT6 residue Gly60 is pivotal for deacetylation; indeed, the G60A mutant has its deacetylase activity abolished while retaining deacetylase activity. Mechanistically, Gly60 is crucial for NAD⁺ binding, and fatty-acylated substrates, but not acetylated ones, are able to reverse the conformational change induced by its mutation.³⁰ This is in line with the above-mentioned activation of SIRT6-mediated deacetylation in the presence of FFA.^{20,21}

Beyond deacetylation and deacylation, SIRT6 also catalyzes mono-ADP-ribosylation. This was initially demonstrated using

mouse SIRT6 (mSIRT6), which was shown to self-mono-ADP-ribosylate, and suggested that SIRT6 may self-modulate its activity through this post-translational modification (PTM).⁴ Further studies indicated that SIRT6 mono-ADP-ribosylates different factors, including the poly(ADP-ribose) polymerase 1 (PARP1),³¹ the transcription factor KAP1,³² the BAF chromatin remodeling complex subunit BAF170,³³ and the histone lysine demethylase KDM2A.³⁴

Given its peculiar structure, SIRT6 can bind NAD⁺ before the acylated protein, and following binding of both substrates, a slow conformational change allows the formation of the alkylimidate intermediate (Figure 2C, step I). The rate of this step is enhanced by FFA and small molecules and has been shown to be faster during demyristoylation.²¹ This reaction consists of a nucleophilic attack of the acyl carbonyl on C1' of nicotinamide-bound ribose and consequent formation of a C1'-O-alkylimidate intermediate, along with release of nicotinamide. Subsequently, His133 acts as a general base on ribose C3' thereby triggering an intramolecular nucleophilic attack of the C2' hydroxyl toward the C1'-O-alkylimidate, thus yielding the C1'-C2' cyclic intermediate (Figure 2C, step II). A conserved water molecule then catalyzes the hydrolysis of the cyclic intermediate, affording the tetrahedral intermediate (Figure 2C, step III). The imino group then attacks His133, which is now positively charged, thus gaining a proton and resulting in the cleavage of the C-N bond. This leads to the final products O-acyl-ADP-ribose and deacetylated lysine (Figure 2C, step IV), which are then released from the enzyme (Figure 2C, step V).^{3,21}

■ BIOLOGICAL FUNCTIONS AND DISEASE RELEVANCE OF SIRT6

Genome Maintenance. Initial observations on SIRT6-knockout mice revealed hypersensitivity to DNA-damaging agents and genomic instability, indicating aberrant functioning of DNA double-strand break (DSB) repair and base excision repair (BER) mechanisms.³⁵ Following these early studies, a growing body of reports indicated that SIRT6 associates with damaged chromatin sites³⁶ and coordinates the recruitment of different factors to initiate DNA-damage repair (DDR).³⁶⁻³⁹ In particular, Onn and colleagues suggested that a SIRT6 dimer is able to directly bind to open-ended DSBs, whereby each monomer interacts with one DNA strand.⁴⁰

SIRT6-mediated recruitment of repair factors is triggered by the deacetylation of nucleosomes. For instance, H3K56 deacetylation facilitates the recruitment of the ISWI-chromatin remodeller SNF2H, which increases chromatin accessibility, thereby promoting the binding to damaged DNA of repair factors such as BRCA1, RPA, and 53BP1.³⁷ Remarkably, a recent study indicated the crucial role of the SIRT6-SNF2H dimer at the neurological level. Indeed, animals lacking SIRT6 in the brain showed AD symptoms, including increased levels of hyperphosphorylated Tau protein.⁴¹

Recent studies indicated that SIRT6 is phosphorylated on Ser10 by *c-Jun* N-terminal kinase (JNK) under oxidative stress conditions. This PTM enables the binding of SIRT6 to DSBs and subsequent recruitment of PARP1, which mediates nonhomologous end-joining (NHEJ) and homology-directed repair (HDR). PARP1 is also mono-ADP-ribosylated by SIRT6 on Lys521,³¹ a modification that is required for PARP1 activity in BER. In addition, mono-ADP ribosylation of the histone lysine demethylase KDM2A has been shown to augment H3K36me2 level at DNA-damage sites, thereby promoting

H3K9 trimethylation and consequent recruitment of NHEJ factors to DSBs (Figure 3).³⁴

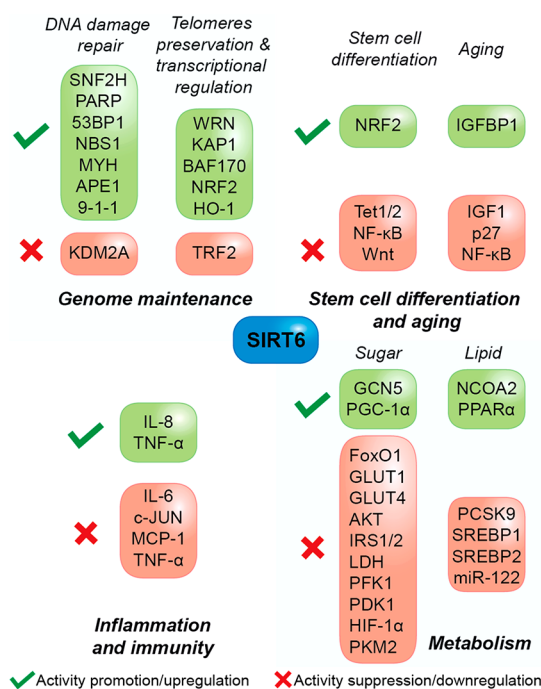


Figure 3. Roles of SIRT6 in cellular and organism homeostasis. The figure indicates the main proteins involved in the most important processes regulated by SIRT6, except cancer.

As anticipated above, the role of SIRT6 in DNA repair has implications in pathology and therapy, particularly in neurodegeneration as the frequency and precision of repair mechanisms declines with age. Accordingly, SIRT6 levels have been shown to decrease with cellular senescence and its overexpression is able to stimulate HDR through the PARP1 pathway.

SIRT6 mediates DNA repair also through BER as indicated by reports showing that overexpression of SIRT6 increases 2-fold the efficiency of this DNA repair mechanism.⁴² Moreover, under oxidative DNA damage, SIRT6 interacts with and stimulates MYH DNA glycosylase and the endonuclease APE1, two enzymes involved in BER. The process is aided by the checkpoint clamp Rad9-Rad1-Hus1 (9-1-1), which forms a multiprotein complex with MYH, APE1, and SIRT6 that is pivotal for whole genome and telomere stability in mammalian cells (Figure 3).⁴³

SIRT6 is also responsible for telomeric preservation in mammalian cells through deacetylation of H3K9 and H3K56 in telomeric regions.^{15,16} SIRT6-mediated H3K9 deacetylation determines chromatin conformational changes that allow the binding of the Werner syndrome ATP-dependent helicase (WRN), the DNA-processing factor that is mutated in the Werner syndrome, a premature aging disorder.¹⁵ Furthermore, SIRT6 interacts with telomere repeat binding factor 2 (TRF2), a pivotal regulator of telomere homeostasis and DNA-damage response, and their interaction is increased during DNA-damage events, in a PARP1-dependent manner. SIRT6 catalyzes TRF2 deacetylation, triggering its ubiquitination finally leading to its proteolysis. In line with this, the levels of the two proteins were negatively correlated in a cohort of colorectal cancer (CRC) patients. These results indicate a regulation mechanism of TRF2

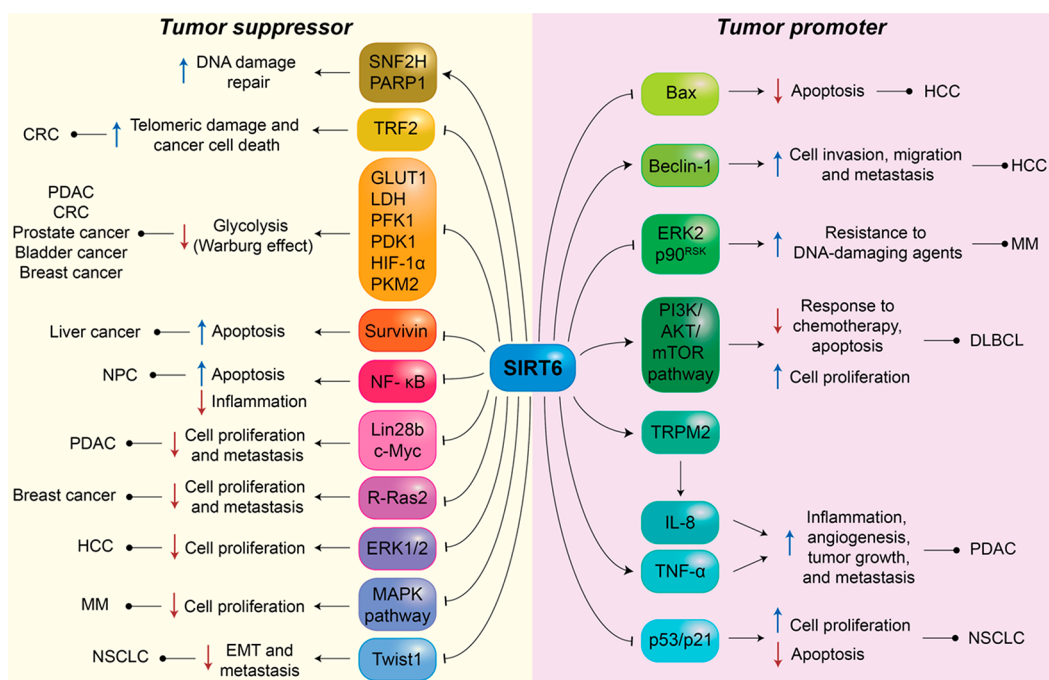


Figure 4. Roles of SIRT6 in cancer. The figure indicates the main factors modulated by SIRT6 in the context of both tumor suppression and promotion. Different mechanisms are involved, including the regulation of DNA-damage response, glycolysis, apoptosis, cell migration, and inflammation.

levels in response to DNA damage and oncogenesis, whereby SIRT6-induced degradation of TRF2 impairs DNA-damage repair leading to cancer cell death.⁴⁴

Apart from its roles in DNA repair and telomeres, SIRT6 is mainly responsible for transcriptional silencing. SIRT6-mediated H3K9 and H3K56 deacetylation contributes to the repression of proteins involved in lipid metabolism, inflammation (NF- κ B-dependent proteins), as well as c-Myc targets, ribosomal proteins, and early developmental genes.^{8,45–47} Furthermore, SIRT6 promotes the silencing of long interspersed element-1 (LINE-1) retrotransposable elements (RTEs), a class of retrotransposons linked to mutagenesis and genomic instability.⁴⁸ SIRT6 facilitates heterochromatin packaging of these RTEs, hence suppressing transposition. Notably, recent findings indicate that this function is directed by SIRT6-mediated mono-ADP-ribosylation of the transcriptional co-repressor KAP1 (Figure 3).³²

Moreover, SIRT6 is responsible for pericentric chromatin silencing through H3K18 deacetylation, and this function is mediated by KAP1, although in a different manner compared to LINE-1 RTEs. Evidence indicates that H3K18 deacetylation is necessary for KAP1 retention at pericentric satellite repeats and consequent transcriptional repression. Conversely, SIRT6 knockout and consequent H3K18 hyperacetylation causes KAP1 detachment and transcriptional derepression.¹⁸ SIRT6-deficient cells display accumulation of pathological pericentric transcripts causing genomic instability, mitotic errors, and cellular senescence, defects associated with aging and tumorigenesis.

As previously mentioned, SIRT6 has also been indicated to catalyze the ADP-ribosylation of the BAF chromatin remodeling complex subunit BAF170 at Lys312. This modification enhances the transcription upon oxidative stress of a subset of the nuclear factor erythroid 2-related factor (NRF2) responsive genes such as HO-1.³³

Stem Cell Differentiation. Embryonic stem cell (ESC) pluripotency maintenance is guaranteed by the expression of Oct4, Sox2, and Nanog genes, which are lost upon differentiation.^{49,50} Recent studies indicated that SIRT6 mediates ESC differentiation through H3K9 and H3K56 deacetylation, which determines the repression of ten-eleven translocation methylcytosine dioxygenase 1 and 2 (TET1 and TET2). These enzymes convert 5-methylcytosine (5-mC) into 5-hydroxymethylcytosine (5-hmC) and regulate cell lineage choice during ESC differentiation (Figure 3).⁵¹

SIRT6 has also a role in mesenchymal stem cell (MSC) and hematopoietic stem cell (HSC) homeostasis through H3K56 deacetylation. Through this activity, SIRT6 seems to coactivate transcription of NRF2 target genes and protect MSCs from oxidative stress.⁵² In addition, SIRT6-mediated H3K56 deacetylation was shown to suppress the NF- κ B signaling pathway, thereby promoting osteogenic differentiation and new bone formation and repair in rats.⁵³ In case of HSCs, SIRT6 interacts with LEF1 and, through H3K56 deacetylation, corepresses Wnt target genes, thus blocking aberrant HSC proliferation.⁵⁴

In addition, SIRT6 expression is associated with higher reprogramming efficiency of induced pluripotent stem cells (iPSCs).⁵⁵ Given the increasing evidence supporting iPSC-based therapies in the context of neurodegenerative diseases, SIRT6 activation may represent a useful strategy to increase the success rate of these treatments.

Aging. Given its roles in genomic maintenance and stem cell homeostasis, SIRT6 has an indirect influence on aging, a process tightly related to DNA damage, telomere maintenance, and differentiation. In addition, SIRT6 plays a direct role in senescence and aging-related conditions through its activity on specific substrates at both the cytoplasmic and nuclear level.

SIRT6 overexpression determined a 15% increase of male mice life expectancy along with reduction of insulin-like growth

factor 1 (IGF1) signaling through increased levels of IGF-binding protein 1 (IGFBP1) and altered phosphorylation of proteins involved in IGF1 downstream signaling.⁷ Moreover, SIRT6 deacetylates the cyclin-dependent kinase inhibitor p27, a factor involved in cellular senescence, hence promoting its proteasome-dependent degradation.⁵⁶ Similarly, the transcription factor NF- κ B, which induces the expression of aging-related genes, is negatively regulated by SIRT6 through a double mechanism. Indeed, at the transcriptional level, SIRT6 deacetylates H3K9 at NF- κ B promoters, thereby reducing the expression of its components, while at the protein level, SIRT6 catalyzed deacetylation of the NF- κ B p65 subunit (RelA) at Lys310 results in NF- κ B nuclear export (Figure 3).⁵⁷

Cancer. DNA damage and cell cycle dysregulation are two of the most important hallmarks of cancer; hence, it comes with no surprise that SIRT6 has been regarded as a tumor suppressor, as indicated by early studies in knockout mice showing genomic instability.⁶ Further investigations indicated that SIRT6 knockout in MEFs leads to tumorigenesis without activation of known oncogenes, and deletion of SIRT6 *in vivo* correlates with an increased number, size, and aggressiveness of tumors (Figure 4).^{8,11} The tumor-suppressor role of SIRT6 was associated with the suppression of glycolytic genes crucial for the Warburg effect, a metabolic shift common in cancer cells where ATP is obtained mostly through glycolysis rather than mitochondrial oxidative phosphorylation, in order to generate immediate energy to support fast proliferation and related cellular processes.⁵⁸ These genes, including the glucose transporter-1 (GLUT1), lactate dehydrogenase (LDH), phosphofructokinase-1 (PFK1), and pyruvate dehydrogenase kinase-1 (PDK1), are regulated by the hypoxia-inducible factor 1 α (HIF-1 α), which is corepressed by SIRT6.⁵⁹ SIRT6 also deacetylates pyruvate kinase M2 (PKM2), a nuclear isozyme that enhances aerobic glycolysis even under hypoxia conditions and promotes tumor growth. SIRT6-mediated deacetylation triggers PKM2 transport to the cytoplasm and repression of its functions.⁶⁰ In addition, glycolytic genes are downregulated through direct deacetylation of H3K9 at their promoters.⁵⁹

In line with this, SIRT6 is selectively downregulated in CRC and pancreatic ductal adenocarcinoma (PDAC), which display increased expression of glycolysis-related genes.⁸ The following studies confirmed these findings and expanded the role of SIRT6 as a main regulator of glycolysis in prostate, bladder,⁶¹ and breast cancers.⁶² Interestingly, SIRT6 activity is antagonized by the Runt-related transcription factor 2 (RUNX2), which represses SIRT6 transcription in low-glucose conditions.⁶² In addition, E2 transcription factor 1 (E2F1) negatively regulates SIRT6 in response to hypoxia, hence facilitating the Warburg effect.⁶¹

SIRT6-mediated H3K9 deacetylation has effects on multiple oncogenes beyond glycolytic genes. These include two proteins involved in apoptosis inhibition and consequently tumor progression: the caspase activation inhibitor survivin⁶³ and the RNA-binding oncofetal protein Lin28b.⁶⁴ Liver cancer mouse models also showed that survivin activity is impaired through the inhibition of NF- κ B activation and consequent binding to a survivin promoter.⁶⁵ NF- κ B is also involved in the activation of other antiapoptotic proteins (FLIP, c-IAP1/2, and XIAP)⁶⁶ and its expression is antagonized by SIRT6 in nasopharyngeal carcinoma (NPC).⁶⁷ Lin28b expression is downregulated through deacetylation of both H3K9 and H3K56. In PDAC, SIRT6 deficiency was associated with H3K9 and H3K56 hyperacetylation at the Lin28b promoter and poor patient prognosis; moreover, in a mouse model of pancreatic cancer, a

SIRT6 deficit led to increased tumor aggressiveness and metastasis.⁶⁸ Given the severity of PDAC and the important role played by SIRT6 in this subset of tumors, targeting this pathway through activation of SIRT6 may represent a successful approach for this type of malignancy.

Lin28b is also a target gene of the c-Myc oncogene. In PDAC, Lin28b promoter hyperacetylation is associated with c-Myc recruitment and consequent augmentation of cancer progression and metastasis.⁶⁸ Notably, c-Myc activity is antagonized by SIRT6, which represses the transcription of c-Myc and its target genes and leads to cell cycle arrest and inhibition of tumor growth.^{69,70}

SIRT6 deacylase activity also contributes to its action as a tumor suppressor. Indeed, SIRT6 deacetylates the GTPase R-Ras2, a Ras-family protein that contributes to tumorigenesis and metastasis.²³ SIRT6-mediated deacetylation of R-Ras2 shifts its location toward intracellular vesicles rather than the plasma membrane, where it usually sits, hence blocking its signaling and cell proliferation.²³

Notwithstanding the great number of reports indicating the tumor-suppressor role of SIRT6 in many forms of cancer, some evidence points toward an oncogenic role of SIRT6 under specific conditions (Figure 4). For instance, in hepatocellular carcinoma (HCC), the activity of SIRT6 in DNA-damage repair and cellular senescence prevention play in favor of cancer cell growth.^{71,72} In addition, SIRT6 deacetylates H3K9 at the promoter of the proapoptotic factor Bax, resulting in evasion from apoptosis.⁷³ SIRT6 also facilitates the epithelial–mesenchymal transition (EMT) in HCC through deacetylation of the autophagy regulator Beclin-1 leading to the autophagic degradation of E-cadherin, a crucial receptor involved in cell adhesion.⁷⁴ The controversial role of SIRT6 in cancer is confirmed by a separate study that suggests a protective role of SIRT6 in HCC mediated by the inhibition of ERK1/2 phosphorylation and the suppression of its downstream pathway.⁷⁵

A connection between SIRT6 and MAPK signaling has also been described in multiple myeloma (MM), although at a transcriptional level. In MM, high SIRT6 levels have been associated with poor prognosis. This disease is characterized by high genome instability; hence, SIRT6 overexpression may be a compensatory response to facilitate DNA repair. While this mechanism may be favorable for cancer cell survival, Cea and colleagues demonstrated that in MM cells, SIRT6 interacts with ELK1 and deacetylates H3K9 at the promoters of MAPK signaling genes, thus stopping cell proliferation. On the other hand, SIRT6-mediated suppression of ERK2 and p90^{RSK} signaling increases resistance to DNA-damaging therapeutics.⁷⁶ Upregulation of SIRT6 has also been observed in other blood cancers, including acute myeloid leukemia,⁷⁷ chronic lymphocytic leukemia,⁷⁸ and diffuse large B-cell lymphoma (DLBCL).⁷⁹ In DLBCL cells, knockdown of SIRT6 leads to higher sensitivity to chemotherapy, altered cell proliferation, augmented rates of apoptosis, and cell cycle arrest. These phenotypes were associated with inhibition of the PI3K/AKT/mTOR signaling pathway.⁷⁹

SIRT6 catalytic activity determines an increase of the intracellular ADP–ribose concentration, which activates the Ca²⁺ channel TRPM2. Increased Ca²⁺ concentration finally leads to the activation of the Ca²⁺-dependent nuclear factor of activated T cells (NFAT), which upregulates the expression of TNF- α and IL-8, two proangiogenic and proinflammatory cytokines that promote tumor growth and metastasis.⁸⁰

Table 1. Most Relevant SIRT6 Activators

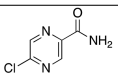
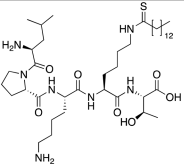
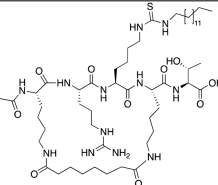
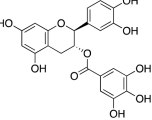
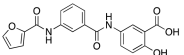
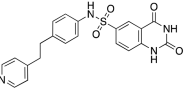
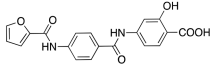
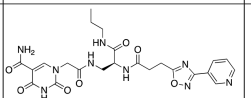
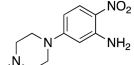
Compound	Structure	Effect on SIRT6 activity	Cellular and <i>in vivo</i> effects	Ref
1a Myristic acid		EC ₅₀ = 246 μM ×10.8 max activation (deacetylation)	-	20
2b OEA		EC ₅₀ = 3.1 μM ×2.1 max activation (deacetylation)	-	102
3e Cyanidin		EC ₅₀ = 460 μM ×55 max activation (deacetylation)	In Caco-2 cells: dose-dependent SIRT6 upregulation; increased expression of FoxO3α. Decreased expression of Twist1 and GLUT1.	103
5 UB3039		EC ₅₀ = 38 μM ×3.5 max activation (deacetylation)	SIRT6 activation in NSCLC, colon and epithelial cervix carcinoma, and fibrosarcoma. Decrease of H3K9 and H3K56 acetylation and autophagy-related cell death.	124, 125
7a MDL-800		EC ₅₀ = 10.3 μM ×22 max activation (deacetylation)	Dose-dependent decrease of H3K9Ac and H3K56Ac in HCC and NSCLC causing cell cycle arrest. HCC tumor growth suppressed also in mouse xenograft models.	128, 129
7c MDL-811		EC ₅₀ = 5.7 μM (deacetylation)	Dose-dependent reduction of H3K9Ac, H3K18Ac, and H3K56Ac levels in different CRC cell lines and antiproliferative effects associated with marked G0/G1 cell cycle arrest. CRC growth suppressed also in patient-derived organoids and antitumor efficacy in cell line-derived and patient-derived xenografts.	132
8b CL5D		EC ₅₀ = 15.5 μM (deacetylation) ×50 increase in <i>k_{cat}/K_m</i> <i>K_i</i> = 13.4 μM (demyristoylation)	Time-dependent SIRT6 deacetylase activity enhancement in full length histones extracted from HEK293T cells	3
10b		EC ₅₀ = 5.35 μM (deacetylation) EC ₅₀ = 8.91 μM (demyristoylation)	Rise in SIRT6 melting temperature at 25 μM (CETSA). Suppression of PDAC cells proliferation cell cycle arrest in G2. Antitumor activity in a human pancreatic tumor xenograft mouse model associated with decrease of H3K9 acetylation levels.	138

A recent study indicated that SIRT6 is overexpressed in NSCLC cells, and its silencing determined activation of the p53/p21 pathway and consequent inhibition of cell proliferation associated with cell cycle arrest and apoptosis.⁸¹ Conversely, an earlier study indicated that SIRT6 suppresses NSCLC

proliferation through inhibition of Twist1 expression, a factor that facilitates EMT and metastasis.⁸²

These examples indicate the complicated role played by SIRT6 in tumorigenesis, suggesting a context dependency. If we take into account the involvement of SIRT6 in DNA-damage

Table 2. Most Relevant SIRT6 Inhibitors

Compound	Structure	Effect on SIRT6 activity	Cellular and <i>in vivo</i> effects	Ref
11c 5-Cl-PZA		IC ₅₀ = 33.2 μM (deacetylation)	-	150
14b BHJH-TM3		IC ₅₀ = 8.1 μM (demyristoylation)	SIRT6 inhibition and increased TNFα fatty acylation in HEK293T cells.	154
15f		IC ₅₀ = 0.319 μM (demyristoylation)	No effects, likely because of poor permeability.	155
17a Catechin gallate		IC ₅₀ = 2.50 μM (deacetylation)	-	103, 104
19b OSS_128167		IC ₅₀ = 89 μM (deacetylation)	Augmented H3K9 acetylation and TNF-α secretion in BxPC3 cells. GLUT1 upregulation and increased glucose uptake in L6 rat myoblasts and BxPC3 cells. Improved glucose tolerance and reduced plasma levels of insulin, triglycerides, and cholesterol in a murine model of type 2 diabetes. Sensitization of MM to DNA-damaging chemotherapeutics. Decreased viability and proliferation inhibition of DLBCL cells. Reduced tumor growth and Ki-67 levels in mouse xenograft.	79, 163, 164, 165
20b		IC ₅₀ = 37 μM (deacetylation)	Increased H3K9 acetylation in BxPC3. Augmented glucose uptake in L6 rat myoblasts and BxPC3 cells. Sensitization of BxPC3 cells to gemcitabine. Enhancement of olaparib anticancer activity in Capan-1 cells.	166, 167
21b		IC ₅₀ = 22 μM (deacetylation)	Increased H3K9 acetylation and glucose uptake in PBMCs. Impaired TNF-α secretion and T lymphocyte proliferation. Sensitization of pancreatic cancer cells to gemcitabine.	168
22a A127-(CONHPr)-B178		IC ₅₀ = 6.7 μM (demyristoylation)	Increase of DNA-damage markers and telomere-dysfunction induced foci in HUVECs. Reduction in TNF-α levels.	169
23		IC ₅₀ = 4.93 μM (deacetylation)	Dose-dependent increase of H3K9 and H3K18 acetylation levels in BxPC-3 cells. Increased GLUT-1 expression levels. Reduction of blood glucose content in a mouse model of type 2 diabetes.	171

repair, depending on the stage of cancer progression, this pathway may have tumor-promoting or tumor-suppressing effects.¹¹ Moreover, high levels of SIRT6 associated with tumors may also represent a compensating response rather than a causality. Therefore, it is vital to distinguish the potential of

SIRT6 as a therapeutic target or as a biomarker in each type of tumor.

Inflammation and Immunity. In the context of immune regulation, SIRT6 has been shown to upregulate proinflammatory cytokines, as explained above in the case of TNF-α and IL-

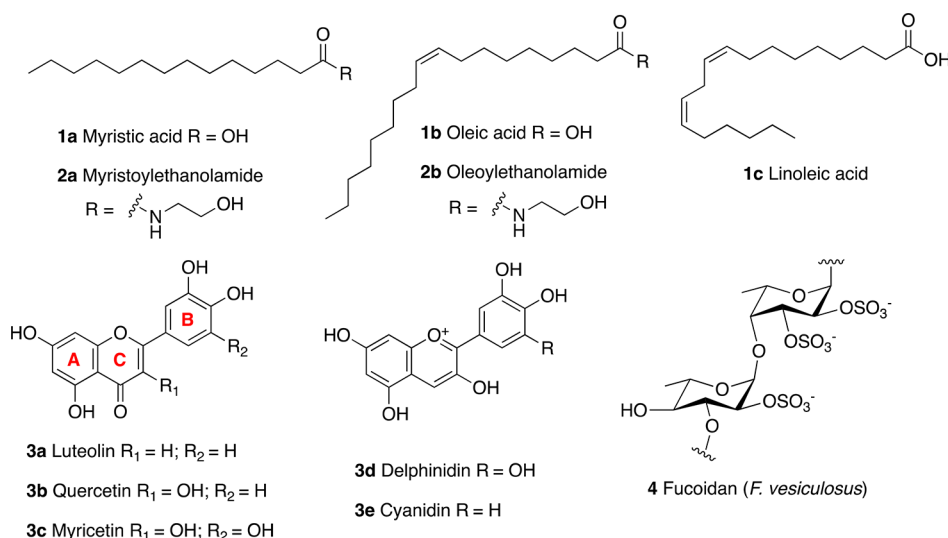


Figure 5. SIRT6 modulators based on endogenous ligands (upper panel) and natural products (lower panel).

8.⁸⁰ SIRT6 catalyzes the demyristoylation of TNF- α at Lys19 and Lys20, triggering its secretion^{22,30} during inflammatory response, while acylated TNF- α is retained and finally degraded in lysosomes. In addition, TNF- α levels are positively regulated by NAD⁺ concentration, and SIRT6 was identified as the mediator of the increased translation efficiency of *Tnf* mRNA.⁸³

On the other hand, SIRT6 also exerts anti-inflammatory roles through negative regulation of NF- κ B, and this is supported by studies in macrophages where SIRT6 deletion promotes NF- κ B activation and IL-6 production.⁸⁴ Studies performed on SIRT6-knockout mice indicated a chronic liver inflammation and fibrosis. Moreover, SIRT6-deficient lymphocytes and myeloid-derived cells presented aberrant activation. Mechanistically, SIRT6 repressed the transcription of genes controlled by the oncogenic transcription factor c-JUN (Figure 3).⁸⁵

Sugar and Lipid Metabolism. SIRT6 is undoubtedly a multitasking protein, and beyond its involvement in DNA maintenance and cancer progression, its main function is probably the regulation of glucose and lipid metabolism. As outlined in the context of cancer, SIRT6 corepresses HIF-1 α and deacetylates H3K9 at glycolytic genes promoters,⁵⁹ thus channeling glucose catabolism from glycolysis toward more energy-efficient pathways (Figure 4). Indeed, SIRT6-knockout mice display increased glycolytic pathway associated with high glucose uptake, increased insulin signaling, and severe hypoglycemia as a compensatory response.^{6,59}

SIRT6 modulates glucose homeostasis also through control of gluconeogenesis. SIRT6 has been found to deacetylate the acetyltransferase general control nonderepressible 5 (GCN5), a regulator of cell cycle progression involved in the onset of different tumors,^{86–88} leading to an increased enzymatic activity. In the liver, increased GCN5 activity results in acetylated PGC-1 α ,⁸⁹ thus leading to reduced gluconeogenesis gene expression,⁹⁰ which prevents hyperglycemia in diabetic/obese mice.⁸⁹ Another important transcription factor for gluconeogenesis is FoxO1, which activates the transcription of the rate-limiting gluconeogenesis enzymes glucose-6-phosphatase (G6PC) and phosphoenolpyruvate carboxykinase (PCK1).⁹¹ FoxO1 is deacetylated by SIRT6, triggering its nuclear export and reduced transcription of its target genes (Figure 3).⁹²

SIRT6 activity has also an effect on insulin signaling through downregulation of glucose transporters GLUT1 and GLUT4

and decreased phosphorylation of AKT,⁹³ an important regulator of cellular glucose uptake.⁹⁴ Mechanistically, SIRT6 is involved in the inactivation of AKT upstream proteins, including the insulin receptor substrates IRS1/2.⁹³ Therefore, the absence of SIRT6 sensitizes the organism to insulin action, giving a complementary explanation to glycolytic gene suppression for the observed hypoglycemia in SIRT6-knockout mice.

In the case of lipid metabolism, SIRT6 reduces triglyceride synthesis and fatty-acid uptake while promoting β -oxidation, as indicated by mice-knockout studies.⁴⁷ SIRT6 also contributes to keeping low the levels of LDL-C (Figure 3).⁹⁵ Mechanistically, SIRT6 has been shown to decrease acetylation of the PPAR α coactivator NCOA2, although it is not clear whether NCOA2 is a direct substrate of SIRT6 enzymatic activity. This determines activation of PPAR α , a key transcription factor for hepatic β -oxidation genes.⁹⁶ Furthermore, SIRT6 represses the expression of the proprotein convertase subtilisin/kexin type 9 (PCSK9), which controls the degradation of LDL-C in lysosomes (Figure 3).⁹⁷ Through interaction with FoxO3 α , SIRT6 is recruited at the PCSK9 promoter, where it deacetylates H3K9 and H3K56, hence suppressing its transcription.⁹⁸ SIRT6 also deacetylates H3K9 and H3K56 at the promoters of genes regulated by the sterol regulatory element-binding protein 1 and 2 (SREBP1/2).⁹⁹ These transcriptional regulators activate transcription of lipogenic genes and are also directly controlled by SIRT6 at the transcriptional level through H3K56 deacetylation at promoters. Notably, micro-RNAs miR-33a and mi33b, which are expressed from the introns of SREBP1/2, are associated with repression of SIRT6 levels, contributing to a negative feedback loop in the SIRT6-SREBP1/2 axis.¹⁰⁰ Another micro-RNA involved in SIRT6-mediated pathways is miR-122, the most abundant hepatic miRNA, which negatively regulates SIRT6 expression and is in turn negatively regulated by SIRT6 (Figure 3). In addition, while SIRT6 positively regulates genes involved in fatty-acid β -oxidation, miR-122 performs an opposite action.¹⁰¹

The connection between SIRT6 activity and fatty-acid metabolism is fascinating given the evidence indicating that FFA are capable of increasing SIRT6 activity *in vitro*.²⁰ Therefore, SIRT6 may act as a fatty-acid sensor that amplifies metabolic signals into epigenetic responses that affect crucial homeostatic mechanisms beyond metabolism itself; these

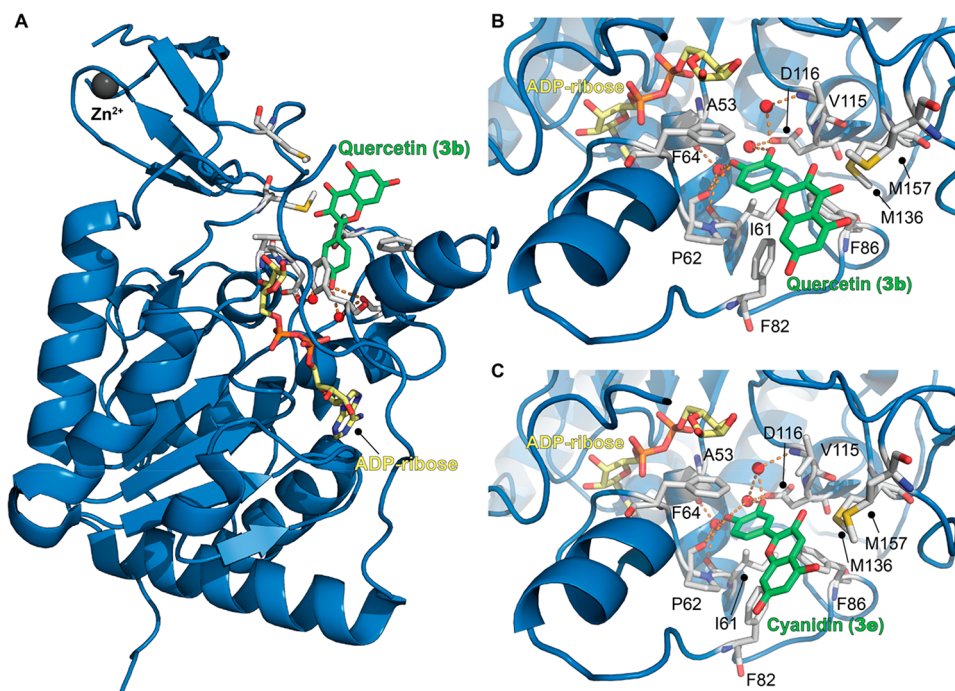


Figure 6. (A) Structure of SIRT6 in complex with ADP-ribose (yellow) and quercetin (**3b**) (PDB ID: 6QCD). (B) Focus on **3b** binding site showing the presence of key water molecules (red spheres) mediating protein-compound interaction. (C) Structure of SIRT6 in complex with ADP-ribose (yellow) and cyanidin (**3e**) with a focus on the **3e** binding site (PDB ID: 6QCH). Key residues for compounds' binding are labeled, and polar interactions are shown as dashed orange lines.

include all the pathways analyzed in this section such as genomic maintenance, immunity, cellular differentiation, and trans-formation.

■ PHARMACOLOGICAL MODULATION OF SIRT6

The implications of SIRT6 as a positive regulator of metabolism and aging, along with the discovery that the deacetylase activity may be enhanced by FFA, has stimulated research groups toward the development of SIRT6 activators (Table 1). On the other hand, given the dual role of SIRT6 in inflammation and cancer, inhibitors have also been developed (Table 2). The possibility of either activating or inhibiting SIRT6 in a context-dependent manner paves the way for personalized pharmacology. From a wider perspective, highly potent and selective SIRT6 modulators (both activators and inhibitors) allow the molecular details of its activity to be better scrutinized and further validate the enzyme as a pharmacological target.

In the following section, we will first discuss the most relevant SIRT6 activators followed by a detailed description of SIRT6 inhibitors.

SIRT6 Activators. As already mentioned, early studies on SIRT6 activity indicated that FFA containing 14 to 18 carbons (Figure 5, upper panel) stimulated SIRT6 activity. In particular, myristic acid (**1a**) increased deacetylase activity up to 10.8 times, with an EC_{50} of $246 \mu\text{M}$ with a 35-fold increase in catalytic efficiency (k_{cat}/K_m value, i.e., the ability of SIRT6 to capture a substrate for catalysis) at $400 \mu\text{M}$, suggesting increased affinity of SIRT6 for the acetylated substrate.²⁶ Oleic (**1b**) and linoleic acid (**1c**) displayed EC_{50} values of 90 and $100 \mu\text{M}$, yielding an increase in deacetylase activity of 5.8 and 6.8 times, respectively. In the same study, **1a** was shown to act as a competitive inhibitor for demyristoylation, suggesting that the same hydrophobic pocket occupied by FFA during deacetylation is necessary to accommodate the long acyl chain of fatty-acid substrates for

deacylation. These findings are the basis for the development of small-molecule SIRT6 activators.²⁰

Following the studies on FFA, it has been shown that myristoylethanolamide (MEA, **2a**) and oleoylethanolamide (OEA, **2b**), the ethanolamine derivatives of **1a** and **1b**, showed a 2-fold maximum activation of SIRT6 and EC_{50} values of 7.5 and $3.1 \mu\text{M}$, respectively.¹⁰² In the same study, **1b** and **1c** were tested, yielding SIRT6 maximum-fold activation of 4.6 and 3.7 along with EC_{50} values of 89 and $230 \mu\text{M}$, respectively. Rahnasto-Rilla et al. also evaluated the influence of the flavonoids luteolin (**3a**) and quercetin (**3b**) on SIRT6 activity. The skeleton of flavonoids consists of a benzene ring (A) fused with a heterocyclic pyran ring (C) presenting a further phenyl group (ring B) in position 2. All the compounds described here present hydroxyl groups on carbons 5 and 7 in ring A (Figure 5, lower panel). **3b** belongs to the subclass of flavonols and are characterized by an oxidized pyran ring, bearing a carbonyl group in position 4 and an additional hydroxyl group in position 3. Differently, **3a** is a flavon and lacks the hydroxyl group in position 3. Both compounds demonstrated a dose-dependent role, whereby they exert inhibitory activity at low concentrations with IC_{50} values of $1.9 \mu\text{M}$ (**3a**) and $24 \mu\text{M}$ (**3b**) while increasing the deacetylase activity at higher concentrations. In particular, **3a** showed a 6-fold maximum activation with an EC_{50} value of $270 \mu\text{M}$, while **3b** yielded 10-fold maximum activation and an EC_{50} of $990 \mu\text{M}$.¹⁰² Although the EC_{50} values for these two flavonoids are very high and with scarce pharmacological relevance, these results suggest multiple binding sites for small molecules, which may interact with an inhibition site at low concentrations while inducing favorable conformational changes that activate the enzyme at higher concentrations.

Following these studies, further flavonoids were tested for their capability of altering SIRT6 enzymatic activity.¹⁰³ The flavonol myricetin (**3c**) has the same structure of **3b** with an

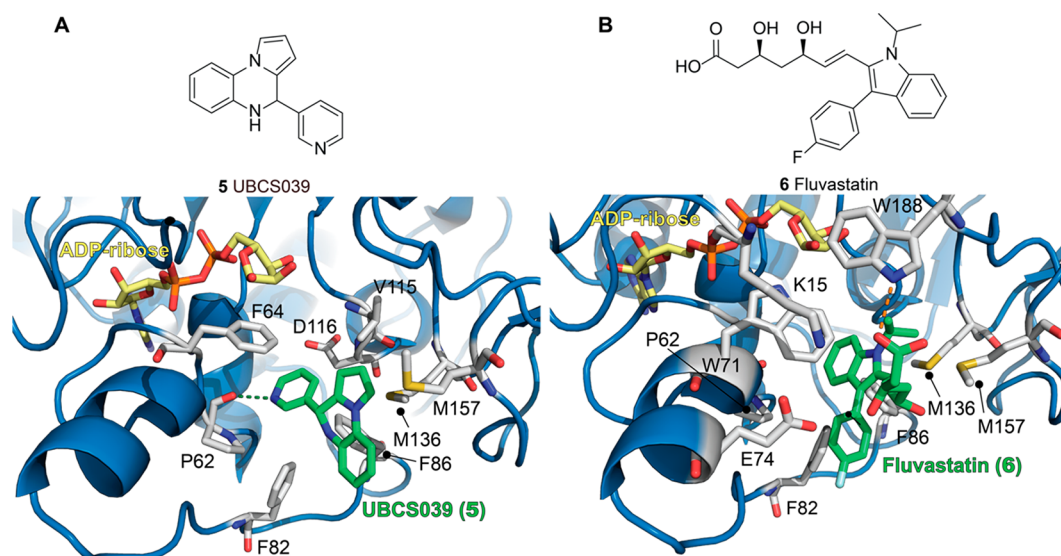


Figure 7. (A) Upper panel: Molecular structure of UBSC039 (5). Lower panel: Structure of SIRT6 in complex with ADP-ribose (yellow) and 5 (green) with a focus on the 5 binding site (PDB ID: 5MF6). (B) Upper panel: Molecular structure of fluvastatin (6). Structure of SIRT6 in complex with ADP-ribose (yellow) and 6 (green) with a focus on the 6 binding site (PDB ID: 6ZU4). Key residues for compounds' binding are labeled, and polar interactions are shown as dashed orange lines.

extra hydroxyl group in 3'. This compound displayed an EC_{50} of 404 μ M and 7.7-fold maximal SIRT6 activation, like observed for 3a.

Anthocyanidins are a subgroup of flavonoids which, compared to flavonols, lack the carbonyl group in position 4 of ring B. Delphinidin (3d), the anthocyanidin analogue of 3c, showed decreased activating potency, with an EC_{50} of 760 μ M and 6.3-fold maximal SIRT6 activation. Remarkably, removal of the 3' hydroxyl group in the case of cyanidin (3e) led to a massive increase in activation efficiency as indicated by the 55-fold maximum activation and EC_{50} of 460 μ M.¹⁰³ Notably, 3e exhibited in-cell effects when tested on colon adenocarcinoma Caco-2 cells, with a dose-dependent SIRT6 upregulation along with modulation of SIRT6-associated genes such as FoxO3a, Twist1, and GLUT1. In particular, the authors observed a dose-dependent increase in FoxO3a expression, while Twist1 and GLUT1 were decreased.

Although the activity of these molecules toward other SIRTs was not assessed in this study, another report evaluated 3b action on SIRT1–3, SIRT5, and SIRT6. In this case, 3b showed a 2-fold maximum SIRT6 activation with an EC_{50} of 1.2 mM, and no inhibition was observed at low concentrations. Conversely, 3b inhibited SIRT1–3 deacetylation activity and SIRT5-mediated desuccinylation in a concentration-dependent manner.¹⁰⁴ In particular, at a 312.5 μ M concentration, the enzymatic activities of SIRT1/2/3/5 were 60–70% compared to the respective controls, while SIRT6 activity was about 150%. Given their polyphenolic nature, flavonoids are known to present pleiotropic activities and have been shown to inhibit a diverse subset of enzymes. Among others, the starch digestive enzyme α -glucosidase is inhibited by compounds 3a–c and 3e^{105–107} with IC_{50} values in the low–mid μ M range, while α -amylase was shown to be inhibited by 3a–c with IC_{50} values of \sim 300 μ M.¹⁰⁵ Moreover, compounds 3a–e have been reported to inhibit topoisomerases I and II^{108–112} and to affect the epigenetic regulation of transcription through inhibition of DNA methyltransferase 1 (DNMT1).^{113,114} 3b was also shown to suppress the activity of other epigenetic enzymes such as

HDAC1¹¹⁵ and the histone acetyltransferase (HAT) p300.¹¹⁶ In contrast, a different study indicated that 3b administration results in increased histone H3 acetylation, associated with HAT activation.¹¹⁷ Moreover, compounds 3a–c have been reported to interfere with multiple bioassays, thus being classified among the pan assay interference compounds (PAINS)^{118,119} and suggesting caution in interpreting the results of biological studies on them.

Nonetheless, flavonoids could represent useful hit compounds for the development of SIRT6 activators thanks to the release of SIRT6–3b and SIRT6–3e cocrystal structures (PDB IDs: 6QCD and 6QCH, respectively). These structures indicated that 3b and 3e interact with SIRT6 at the distal end of the hydrophobic acyl-binding pocket, with surface contacts with the β 6/ α 6 loop that caps this channel (Figure 6).¹⁰⁴ In both cases, the catechol portion (ring B) is inserted in the acyl-binding pocket with the 4'-hydroxyl group forming a hydrogen bond with Pro62 backbone oxygen and with a conserved water molecule that in turn forms a hydrogen bond with the backbone oxygens of Ala53 and Ile61. Similarly, the 3'-hydroxyls of both molecules are hydrogen-bonded with another conserved water molecule that is in contact with the side-chain oxygen of Asp116. In the case of 3b, the chromen-4-one moiety (rings A and C) forms hydrophobic contacts with Phe64/82/86, Val70/115, and Met136/157 (Figure 6B). As for 3e, although the density of this portion was weaker, it was positioned in the same area as 3b, suggesting a similar binding mode.¹⁰⁴ Compared to 3b, 3e lacks the carbonyl group pointing toward Met136/157, which may be one of the reasons for its higher potency. Indeed, this group may represent a steric hindrance, and its absence allows optimal hydrophobic contacts between ring C and Met136/157 (Figure 6C).

The crystal structures of SIRT6 in complex with 3b and 3e enable the identification of key features for ligand binding and, likely, could be exploited to develop new compounds containing only the hydroxyl groups essential for the interaction with the target, thus decreasing the polyphenolic character. Moreover, computational scaffold hopping^{120,121} approaches integrated

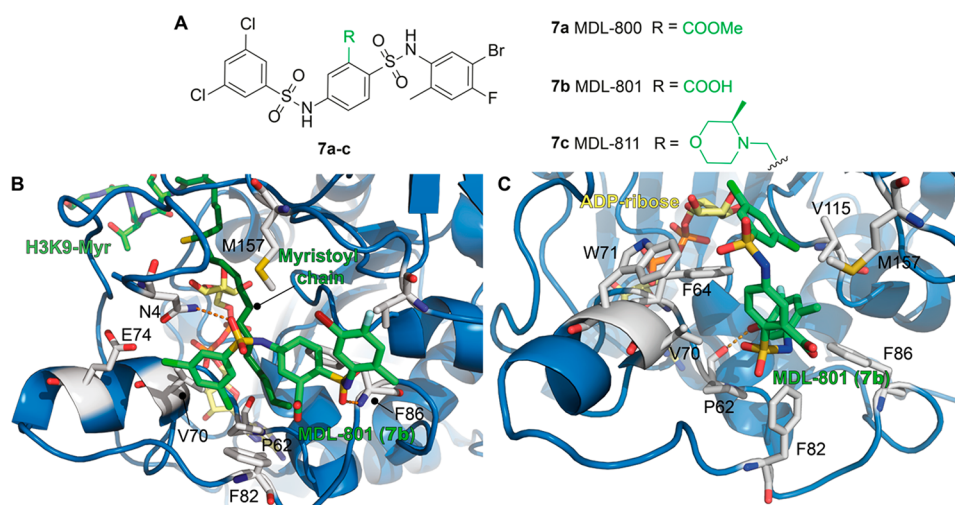


Figure 8. (A) Molecular structures of MDL compounds (7a–c). (B) Structure of SIRT6 in complex with ADP–ribose (yellow), H3K9–Myr (myristoyl chain in dark green), and MDL-801 (7b) (green) with a focus on the 7b binding site, as reported by Huang et al. (PDB ID: 5Y2F). (C) Structure of SIRT6 in complex with ADP–ribose (yellow) as well as 7b (green) with a focus on the 7b binding site, as reported by You and Steegborn (PDB ID: 6XVG). Key residues for compounds' binding are labeled, and polar interactions are shown as dashed orange lines.

with AI-driven drug discovery¹²² could allow the design of derivatives bearing a different core but retaining the moieties important for SIRT6 interaction. Overall, these strategies could enable molecules with increased specificity and potency to be obtained.

Another naturally occurring molecule showing SIRT6 activation is fucoidan (4), a heterogeneous sulfated polysaccharide present in brown algae. Its backbone consists of repeating (1 → 3) or (1 → 3) and (1 → 4) linked α -L-fucopyranose residues, in which some hydroxyl groups form sulfated esters (Figure 5, lower panel).¹²³ The oversulfated fucoidan subtype extracted from *Fucus vesiculosus* displayed a 355-fold increase of SIRT6 activity at a 100 μ g/mL concentration. In addition, when tested against other SIRTs (SIRT1/2/3), it did not display significant changes in activity, suggesting a specific action toward SIRT6. 4 was also able to activate SIRT6 acetylation toward H3K9 *in vitro*. According to the authors of the study, sulfate esters may play a central role in SIRT6–4 interaction and hence SIRT6 activation.¹²³ However, the heterogeneity of the mixture, the polymeric nature of the compound, and the absence of kinetic data makes it difficult to compare this macromolecule to small molecules and to devise structure–activity relationships.

The first synthetic SIRT6 activator is the pyrrolo[1,2-*a*]quinoxaline derivative UBCS039 (5, Figure 7a, upper panel), which exhibited an EC_{50} of 38 μ M and 3.5 maximum activation of SIRT6 in H3K9Ac peptide deacetylation assays.¹²⁴ 5 showed specific binding on SIRT6, with no significant effects on basal SIRT1, 2, and 3 deacetylation activities. Notably, it stimulated SIRT5 desuccinylation activity (2-fold increase at 100 μ M), the physiologically dominant activity of this enzyme. The 5–SIRT6 cocrystal (solved at 1.87 Å resolution, PDB ID: SMF6) indicated a similar binding mode to 3b and 3e, with the compound occupying the exit of the acyl channel pocket and exposing the benzene moiety of the quinoxaline to solvent. The tricyclic portion of the molecule likely forms a methionine–aromatic ring interaction with Met136 along with weak hydrophobic interactions with Trp71, Phe82, Phe86, Ile185, and Met157. In addition, the pyridine nitrogen forms a hydrogen bond with the backbone carbonyl of Pro62 (Figure

7a, lower panel); this interaction represents a key anchoring point as a shift of the position of the nitrogen led to decreased SIRT6 affinity and activation. Comparison of this crystal structure with the cocrystal of SIRT6 and myristoylated peptide indicates that UBCS039 overlaps with the last seven carbons of the myristoyl chain. In addition, comparison with the SIRT6/ADP–ribose/3b cocrystal indicates that the compounds share a similar binding site. The 5 pyridine portion overlaps with 3b catechol moiety, and both engage in the key interaction with Pro62. In addition, the pyrrolo[1,2-*a*]quinoxaline moiety of 5 and the chromen-4-one are involved in similar hydrophobic interactions. One difference relies on the fact that 3b possesses a carbonyl group pointing toward Met136/157, which may impair optimal hydrophobic contacts between the aromatic ring and the methionine residues. Differently, the 5 tricyclic system is positioned in a privileged location for aromatic and hydrophobic interactions with Met136/157, thus explaining its higher potency compared to 3b. Although 5 did not display significant inhibition of SIRT6-mediated demyristoylation, as the binding affinity for the myristoylated peptide is much higher, addition of myristoylated peptide decreased 5 binding by an order of magnitude, thus indicating competition for the same binding site. Compound 5 was also tested using physiological substrates, such as full-length histones extracted from calf thymus and HeLa nucleosomes. In both cases, Western blot analysis indicated H3K18 deacetylation in the presence of 5.¹²⁴ Follow-up studies indicated that 5 causes SIRT6 activation in a different subset of cancer cell lines, including NSCLC, colon and epithelial cervix carcinoma, and fibrosarcoma. 5-mediated SIRT6 activation led to decreased H3K9 and H3K56 acetylation and autophagy-related cell death.¹²⁵ This study represents the first evidence of in-cell small-molecule-mediated SIRT6 activation, suggesting a potential therapeutic exploitation of this activity.

A compound screening for drug repurposing recently identified the HMG-CoA reductase inhibitor fluvastatin (6, Figure 7B, upper panel), already approved for hypercholesterolemia treatment, as a SIRT6 activator.¹²⁶ 6 showed an EC_{50} = 7.1 μ M and decreased H3K9 and H3K56 acetylation in HepG2 cell lines. This effect was accompanied by increased nuclear translocation of SIRT6. In addition, 6 treatment increased levels

of phosphorylated AMPK α , which in turn promoted SREBP1 phosphorylation at Ser372. In addition, cleaved SREBP1 was negatively regulated. These results are in line with previous reports suggesting that SIRT6 overexpression represses SREBP1/2 through the AMPK pathway.⁹⁹ Interestingly, a subsequent study found a much higher EC₅₀ (>250 μ M) for 6-mediated SIRT6 activation, though it could reach 3.5-fold maximum activation at 1 mM.¹²⁷ Compound 6 also displayed weak inhibition of SIRT1/2/3, while it did not affect SIRT5 activity. Nonetheless, the authors managed to cocrystallize 6 with the N-terminally truncated SIRT6 (13–308) and ADP-ribose and solved the structure at 2.46 Å (PDB ID: 6ZU4, Figure 7B, lower panel). 6 interacts with SIRT6 at the exit of its acyl channel in its acid form, rather than lactone, forming a hydrogen bond with Trp188 through its carboxyl group. In addition, the fluorophenyl and isopropyl residues point toward the channel exit, while the heptenoic acid moiety interacts with a surface formed by Lys15, Trp71, and Glu74. The indole moiety has a similar positioning of the pyridine ring of 5,¹²⁴ as it is oriented toward the hydrophobic pocket formed by Phe64/82/86, Ile61, Pro62, and Met136. However, bulky substituents, such as the isopropyl and fluorophenyl groups, obstruct the entrance in the pocket, thereby impairing the key polar interactions with the backbone oxygen of Pro62 seen with 5 and other ligands. In summary, the authors of this study suggest that the initially measured low EC₅₀¹²⁶ may be a result of an assay artifact and that the reported cellular effects may be due to an indirect action of 6.¹²⁷ Nevertheless, the elucidation of the 6 binding mode aids the development of modulators possessing the same core scaffold, but different substituents, in order to maximize polar interactions.

Virtual screening followed by *in vitro* evaluation led to the discovery of a new selective and cellularly active SIRT6 activator, the N-phenyl-4-(phenylsulfonamido)benzenesulfonamide derivative MDL-800 (7a, Figure 8A).¹²⁸ 7a displayed an EC₅₀ value of 10.3 μ M, enhancing SIRT6 activity by more than 22 times (at 100 μ M), using a synthetic acetylated peptide (RHKK-ac-AMC) as a substrate. When tested on SIRT6 using the H3K9Ac peptide (KQTARK-ac-STGGWW), 7a exhibited 18-fold maximal SIRT6 activation. In addition, 7a increased the deacetylation of H3K9 and H3K56 on HeLa-extracted nucleosome substrates in a dose-dependent manner. 7a did not display any effect on the enzymatic activities of SIRT1/3/4 and HDAC1–11 at concentrations up to 50 or 100 μ M. It displayed weak inhibition of SIRT2 (IC₅₀ = 100.4 μ M) and weak activation of SIRT5 (IC₅₀ = 104.6 μ M) and SIRT7 (IC₅₀ = 187.1 μ M). Since the IC₅₀/EC₅₀ values are 10 times (or more) greater than SIRT6 EC₅₀, the compound is considered selective. The analogue MDL-801 (7b), in which the methyl carboxylate ester in position 2 of the central benzenesulfonamide ring is replaced by a carboxylic group (Figure 8A), exhibited overlapping SIRT6 activation features with an EC₅₀ = 5.7 μ M. However, while 7a was highly cell permeable and accumulated in cells, 7b had poor cellular permeability and a high efflux ratio. Therefore, the only compound tested for cellular activity was 7a. This molecule caused a dose-dependent decrease of H3K9Ac and H3K56Ac in HCC cells (specifically Bel7405, PLC/PRF/5, and Bel7402 cell lines), leading to inhibition of their proliferation through SIRT6-mediated cell cycle arrest. In particular, the observed IC₅₀ for cell growth (IC_{50-growth}) was between 18.6 and 24 μ M, depending on the cell line. These results were confirmed in mouse xenograft models, where 7a suppressed HCC tumor growth through SIRT6 activation. A recent investigation indicated that 7a

inhibits the proliferation of 12 NSCLC cell lines in a dose-dependent manner and caused cell cycle arrest at the G₀/G₁ phase in NSCLC HCC827 and PC9 cells, consistent with studies indicating the role of SIRT6 in cell cycle regulation.^{16,70} Notably, it exhibited synergistic activity with epidermal growth factor receptor tyrosine kinase inhibitors (EGFR-TKIs) in osimertinib-resistant HCC827 and PC9 cells and in patient-derived primary tumor cells. Moreover, 7a suppressed tumor growth in HCC827 cell-derived xenograft nude mice and caused H3 deacetylation and downregulation of p-MEK and p-ERK in tumor tissues.¹²⁹

Huang et al. solved the cocrystal structure of the complex formed by SIRT6, ADP-ribose, H3K9 myristoylated peptide, and 7b (PDB ID: 5Y2F, Figure 8B).¹²⁸ Given the structural similarities between 7b and 7a, the observed features are likely shared between the two compounds. Interestingly, 7b appeared to interact with SIRT6 in a unique pocket, distinct from the binding site of 3b, 3e, 5, and 6 located in the acyl-binding hydrophobic channel. Indeed, 7b was shown to interact with a surface-exposed distal region defined by the N-terminal residues 1–7, Val70, Glu74, Phe82, Phe86, Val153, and Met157. The 3,5-dichlorobenzene moiety of 7b is involved in weak polar interactions with Asn40, Val70, and Glu74 and engages π -stacking interactions with Phe82 (Figure 8B). The central 2-carboxybenzenesulfonamide ring is also involved in π -stacking interactions with Phe86, whose importance was confirmed by single-residue mutation experiments showing decreased potency of both 7a and 7b toward SIRT6-F86A.¹²⁸ However, a recent report from You and Steegborn argued that the observed electron density could be attributed to a molecule of morpholinoethanesulfonic acid (MES), used as crystallization buffer, rather than 7b.¹³⁰ Therefore, they determined new crystal structures for SIRT6 in complex with 7b. They solved the cocrystal of N-terminal truncated SIRT6_{13–308} in complex with ADP-ribose and 7b (PDB ID: 6XV1) as well as in the absence of 7b (PDB ID: 6XUY). Similarly, they solved the structure for SIRT6_{3–308} (comprising the N-terminus) in complex with ADP-ribose and 7b (PDB ID: 6XVG, Figure 8C), along with a reference structure without the activator (PDB ID: 6XV6).¹³⁰ These structures indicate a different binding mode for 7b, which does not bind at the distal end of the acyl-binding hydrophobic channel but in the same region as the previously described activators 3b, 3e, and 5. In both SIRT6_{13–308}–7b and SIRT6_{3–308}–7b structures, the activator engages in extensive hydrophobic interactions, the central 2-carboxybenzenesulfonamide is packed between Val70, Trp71, and Met157, and the 5-bromo-4-fluoro-2-methylaniline portion interacts with Phe64, Val70, Phe82, Phe86, and Val115. In addition, bromine forms a halogen bond with the backbone amide oxygen of Pro62, which has been shown to be a key residue for small-molecule interactions with SIRT6 (Figure 8C). Notably, the interaction with Pro62 is missing in the binding mode illustrated by Huang et al.¹²⁸ The 3,5-dichlorobenzene moiety is less defined and seems to be largely solvent-exposed. Hence, the structures from the two groups display rather different binding modes for 7b, whose orientations within SIRT6 are perpendicular to each other in the two studies. In response to this report, Huang et al. crystallized SIRT6 with and without 7b using the same conditions as in their original publication (PDB ID: 7CL0 for SIRT6 in complex with ADP-ribose and H3K9 myristoyl peptide; PDB ID: 7CL1 for SIRT6 in complex with ADP-ribose, H3K9 myristoyl peptide, and MDL-801).^{128,131} They showed that, in the absence of 7b, the buffer molecule MES does

not fit properly the originally proposed ligand-binding pocket. In addition, the newly solved cocrystal in the presence of **7b**, although possessing lower overall resolution (3.2 Å for 7CL1 vs 2.53 Å for SY2F), has better electron density for the activator and confirms their initial findings.¹³¹ Importantly, Huang et al. crystallized SIRT6 in the presence of the H3K9 myristoyl peptide, which is absent in the crystallization mixture of You and Steegborn. Overall, the observed differences in the **7b** binding mode may be ascribed to the presence of the substrate, which influences the interaction between the small molecule and SIRT6. Indeed, the crystal structure represents just a conformational state of the protein, whose conformational dynamics can be altered by the presence of ligands, thereby leading to alteration of key interactions between a small molecule and their target. Hence, structures of SIRT6–**7b** from both groups may be equally valid and represent two different states of the protein, regulated by the presence of substrate. Nonetheless, further experiments, including the structure of **7b** in the presence of acetylated substrate may help to further clarify this controversy.

The replacement of the methyl carboxylate with an *N*-methyl-3-methylmorpholine at the C3 position of the central benzene ring of **7a** led to compound MDL-811 (**7c**, Figure 8AA) with improved activity ($EC_{50} = 5.7 \mu\text{M}$) and bioavailability in C57BL/6J mice ($F\%_{\text{MDL-800}} = 71.33\%$ vs $F\%_{\text{MDL-811}} = 92.96\%$).¹³² The improved activity may be explained by the higher number of interactions that the *N*-methyl-3-methylmorpholine moiety can establish. Indeed, it presents an exposed oxygen that can act as a hydrogen bond acceptor and a methyl group potentially involved in hydrophobic interactions. The compound enhanced deacetylation of H3K9, H3K18, and H3K56 in nucleosomes extracted from HeLa cells as well as in HEK293T cells in a dose-dependent manner. **7c** was shown to be specific for SIRT6, as it was not able to affect the activity of SIRT1–3, SIRT5, SIRT7, and HDAC1–11 at concentrations up to 100 μM . According to docking studies, the 3-methylmorpholine moiety may participate in hydrophobic interactions with Phe82, Thr85, and Phe86 of SIRT6, and the oxygen can form a hydrogen bond with the backbone amide of Phe86. As already mentioned, CRC is a type of cancer characterized by heavy downregulation of SIRT6.⁸ Notably, **7c** displayed dose-dependent reduction of H3K9Ac, H3K18Ac, and H3K56Ac levels in different CRC cell lines and antiproliferative effects associated with marked G₀/G₁ cell cycle arrest. In line with this, **7c** suppressed CRC growth in patient-derived organoids and showed antitumor efficacy in cell-line-derived and patient-derived xenograft (CDX and PDX, respectively) models as well as in a spontaneous CRC mouse model. Mechanistically, cytochrome P450 family 24 subfamily A member 1 (CYP24A1), which had been previously shown to be aberrantly overexpressed in CRC,^{133,134} was identified as a new target gene of SIRT6. **7c** also exhibited synergistic activity with vitamin D₃ in suppressing CRC proliferation. Interestingly, vitamin D₃ is both a substrate and transcriptional regulator of CYP24A1 and has shown antitumor efficacy in CRC.^{135,136}

Activity-based screening of lipid-like molecules led to the discovery and optimization of CL4 (**8a**), a compound consisting of a 4-carboxyphthalimide conjugated to an *N*-(2-chlorophenyl)2,5-dichlorobenzamide. **8a** displayed an $EC_{50} = 97 \mu\text{M}$ and 17 maximum-fold activation of SIRT6 deacetylase activity. In addition, it displayed selectivity over SIRT1–3 and SIRT5.²¹ Therefore, **8a** represented an ideal lead compound for the development of selective SIRT6 activators. Removal of chlorine atoms from either the 2,5-dichlorophenyl moiety or

both benzene rings led to the suppression of SIRT6 activation, while progressive addition of chlorine restored this ability (Figure 9, upper panel). Finally, addition of a double-

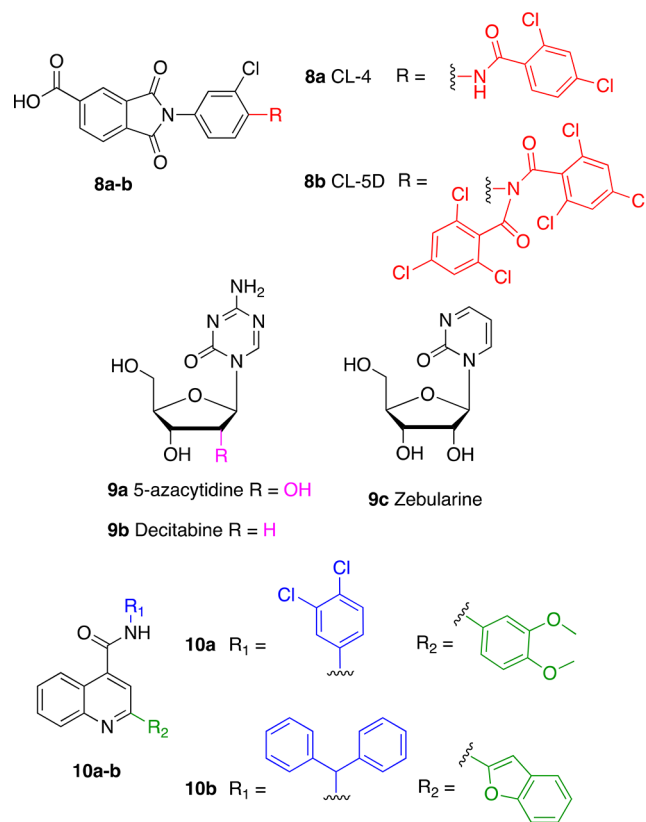


Figure 9. Further synthetic SIRT6 activators.

trichlorobenzoyl group at the aniline nitrogen led to CL5D (**8b**), which showed 7-fold increased potency over **8a**, with an $EC_{50} = 15.5 \mu\text{M}$. Notably, the methyl ester of **8b** did not show any activity. The data obtained from the development of **8b** indicate that electron-withdrawing groups on the aromatic rings are crucial for SIRT6 activation in this series of molecules. In addition, the anionic headgroup (the carboxylic acid) is also essential for activity, and it is probably involved in hydrogen bond interactions. The maximum-fold activation of **8b** was measured in terms of the k_{cat}/K_m ratio, which was ~ 50 under steady-state conditions. **8b** displayed competitive inhibition of demyristoylation ($K_i = 13.4 \mu\text{M}$), suggesting occupation of the acyl-binding pocket, although structural data are missing. **8b** also stimulated SIRT6 deacetylase activity in a time-dependent fashion in full-length histones extracted from HEK293T cells.³

A recent study that evaluated the influence of the FDA-approved DNA hypomethylating agents (DHAs) on sirtuin family members showed that the nucleoside analogues 5-azacytidine (5AC, **9a**), decitabine (DAC, **9b**), and zebularine (**9c**) increase SIRT6 enzymatic activity (Figure 9, middle panel).¹³⁷ **9a** and **9b** increased SIRT6 activity after 12, 24, and 48 h of incubation at 0.25 and 0.5 μM ; albeit, no dose-dependency was observed. Moreover, while the maximum activation (1.3-fold activation) for **9a** was observed after 48 h, **9b** exhibited 1.5-fold activation after 12 h, followed by a decrease in activation efficiency at 24 and 48 h. **9c** could also activate SIRT6 deacetylase activity, although at higher concentrations (0.5 and 1 μM), with 1.4 maximum-fold activation observed after 48 h of

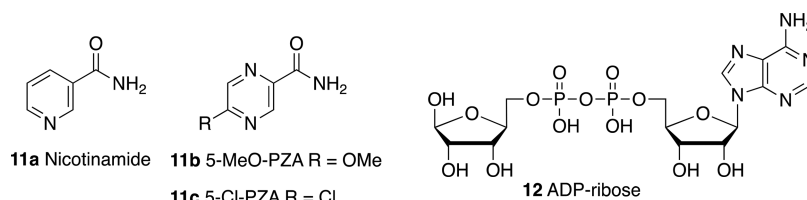


Figure 10. Product-based SIRT6 inhibitors.

incubation. In addition, both **9a** and **9c** (but not **9b**) reduced the enzymatic activity of SIRT1, while the activity of SIRT2, SIRT3, and SIRT5 was not affected by any of these compounds. Although these data indicate that these compounds activate SIRT6, the lack of dose dependency suggests that they have been tested far below their EC₅₀; hence, the maximum activation values presented here should be taken cautiously. In line with these results, U937 leukemia cells treated with 0.5 μM **9b** for 24 and 48 h displayed decreased levels of H3K9Ac and H3K56Ac, according to Western blot experiments. Further ChIP-Seq analysis of bone marrow cells derived from six AML patients and treated with **9b** indicated changes of H3K9 acetylation at 187 gene loci; specifically, 102 genes displayed an acetylation decrease, while 85 genes showed an acetylation increase. The authors of this study speculated that the unexpected increase in acetylation may be a consequence of differential effects of **9b** on both HATs and HDACs or possible upregulation of the HAT enzymes targeting H3K9. Signaling pathway analysis showed that H3K9 acetylation changes are related to pathways like EGF/EGFR and Wnt/Hedgehog/Notch, which are associated with AML. Although the study lacks details about the connection between SIRT6 inhibition and the overall antitumor effect of **9b**, it highlighted a possible second mechanism of action of nucleoside analogues, which is worth exploring. Indeed, these molecules seem to be active at relatively low concentrations; hence, a complete biochemical evaluation by SAR studies may lead to the development of selective SIRT6 inhibitors.

A virtual screening campaign performed using the SIRT6–5 (PDB ID: 5MF6)¹²⁴ complex led to the identification of the initial hit **10a** that was further optimized to provide the 2-(1-benzofuran-2-yl)-N-(diphenylmethyl) quinoline-4-carboxamide (**10b**) as a potent and selective small-molecule activator of SIRT6 (Figure 9, lower panel).¹³⁸ In docking experiments, **10a** appeared to bind at the distal end of the hydrophobic channel and engage in π – π interactions with Phe86 with its quinoline scaffold as well as σ – π interactions with the amide backbone of Ala7 through the 3,4-dichlorobenzene moiety. When tested *in vitro*, compound **10a** increased SIRT6 activity by 50% (EC_{1.5}) at ~27 μM. From the docking model, it appeared that the space around the 3,4-dichlorobenzene group and 3,4-dimethoxybenzene group was not occupied; hence, modifications were executed to add moieties that would strengthen the interactions between the molecule and SIRT6. This led to compound **10b**, where the 3,4-dichlorobenzene and the 3,4-dimethoxybenzene were replaced by a diphenylmethane group and a 2-benzofuranyl moiety, respectively. Compound **10b** displayed activation toward both SIRT6 deacetylase and deacylase activities, with EC₅₀ values of 5.35 and 8.91 μM for deacetylation and demyristoylation, respectively. **10b** showed no influence on the enzymatic activity of SIRT2, SIRT3, SIRT5, and HDAC1–11. It weakly inhibited SIRT1, but the IC₅₀ value for SIRT1-mediated deacetylation (IC₅₀ = 171 μM) is more

than 30 times higher compared to SIRT6 EC₅₀, thereby indicating in any case an appreciable selectivity. According to docking experiments, compound **10b** interacts with SIRT6 in a similar way to its parent compound and presents some extra interactions given by the different substituents. Indeed, the benzofuran forms hydrogen bonds with Met157 and Lys160 and a π – σ interaction with the amide group of Thr156; in addition, the *N*-benzhydryl group is inserted in the allosteric pocket and establishes hydrophobic interactions with Tyr5, Val70, Phe82, Pro62, and Pro80, and one of its benzene rings forms π – π interactions with Phe86. According to this model, although located in a similar region, compound **10b** binds SIRT6 more toward the end of the hydrophobic channel compared to **5**, which may justify **10b**-mediated enhancement of SIRT6 demyristoylation activity. Compound **10b** suppressed the proliferation and caused cell cycle arrest in the G2 phase of PANC-1 and BXPC-3 PDAC cell lines. Cellular thermal shift assay (CETSA)¹³⁹ performed in intact cells confirmed that **10b** (at 25 μM concentration) interacts with SIRT6 in cells. In addition, **10b** exhibited antitumor activity in a human pancreatic tumor xenograft mouse model associated with a decrease of H3K9 acetylation levels. A preliminary study in male Sprague-Dawley rats also indicated a promising pharmacokinetic profile, although the bioavailability was only 4%. Although **10b** with its low micromolar EC₅₀ values is a promising lead compound, we cannot exclude that the effects observed in cells and *in vivo* are related to interactions with off-target proteins beyond SIRT6. Therefore, further functional and target engagement assays such as mass-spectrometry-based thermal profiling,^{140,141} histone deacetylase assay homogeneous (HDASH) procedures,¹⁴² fluorescence resonance energy transfer imaging (FRET) probes,¹⁴² and affinity-based protein profiling (ABPP)¹⁴³ seem necessary to clarify this point. Moreover, genetic studies^{144,145} alone and in combination with compound treatment in both cellular and animal PDAC models would be required to confirm the causal link between the observed phenotypes and SIRT6 activation and to conclusively assess the therapeutic potential of **10b** in this tumor context.

SIRT6 Inhibitors. Given the double-faced involvement of SIRT6 in cancer and inflammation, inhibition of SIRT6 in specific contexts may represent a successful strategy for cancer management. Indeed, inhibitors may target different SIRT6-mediated pathways that contribute to cancer progression such as DNA repair mechanisms, cell differentiation inhibition, and inflammatory response (Table 2).

Nicotinamide (**11a**, Figure 10) is one of the products of the sirtuin-mediated deacylation reaction and may act as a weak product inhibitor of SIRTs without subclass specificity.^{146–148} **11a** has been validated as a SIRT6 deacylation inhibitor through two different assays using H3K9 myristoyl peptides: an HPLC assay yielded an IC₅₀ = 153 μM; similarly in a fluorogenic assay, **11a** displayed an IC₅₀ = 184 μM.¹⁴⁹ In a subsequent study, **11a** displayed an IC₅₀ for a demyristoylation reaction of 73 μM while

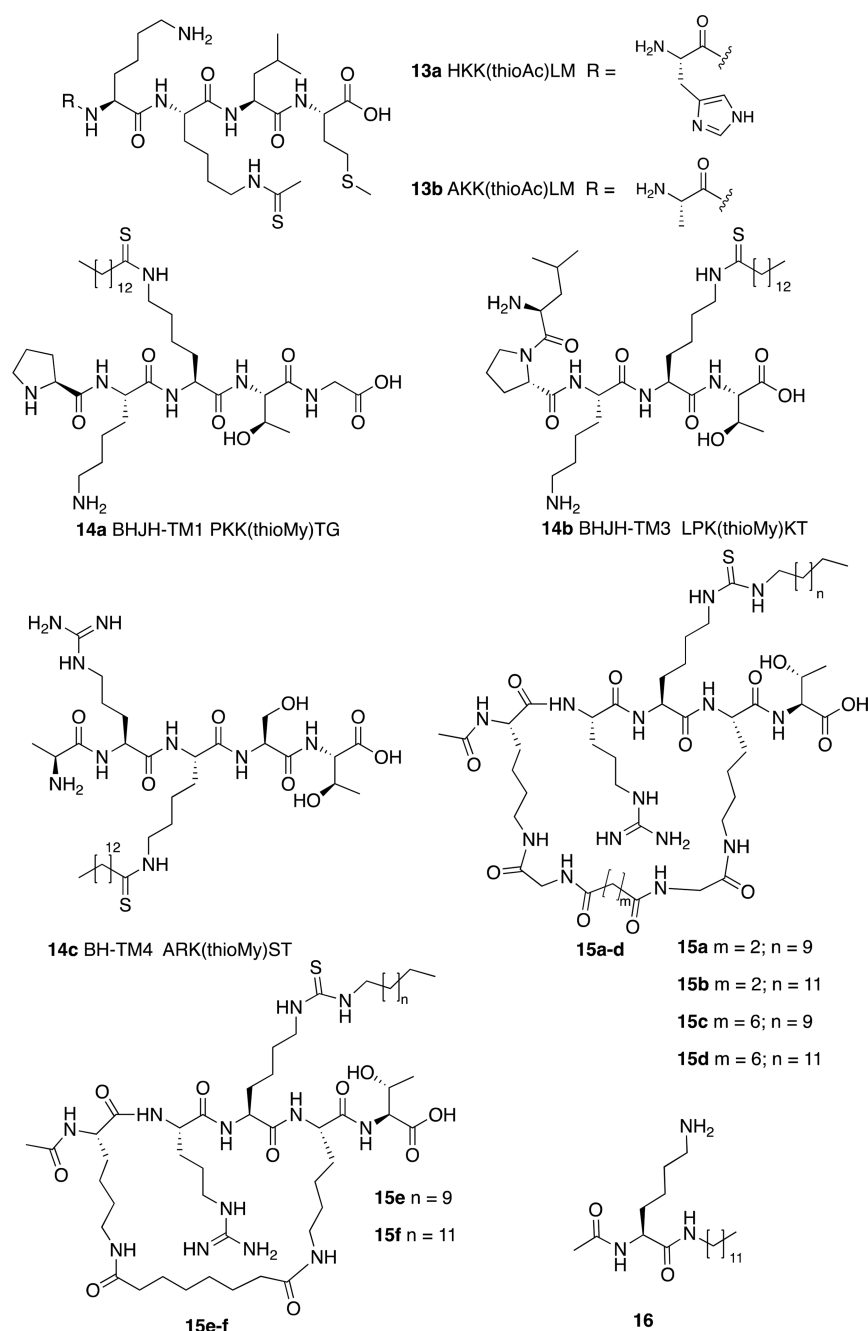


Figure 11. Peptide-based SIRT6 inhibitors.

showing increased inhibitory potency toward deacylation of H3K9 decanoyl peptide ($IC_{50} = 45 \mu M$) and lower potency using H3K9 hexanoyl peptide as a substrate ($IC_{50} = 184 \mu M$).³⁹

Based on the **11a** analogue pyrazinamide (PZA), Bolivar et al. developed two derivatives with improved SIRT6 inhibition activity (Figure 10): 5-MeO-PZA (**11b**, $IC_{50} = 40.4 \mu M$) and 5-Cl-PZA (**11c**, $IC_{50} = 33.2 \mu M$). Remarkably, these compounds did not show NAD^+ competition, hence indicating a different mechanism of action from **11a**.¹⁵⁰ **11c** was reported to be active toward SIRT1, but not SIRT2/3, while **11b** was not evaluated against SIRT1–3. Nonetheless, selectivity against other SIRTs and HDACs need to be ascertained.

ADP-ribose (**12**, Figure 10) also inhibits SIRT6 activity and showed higher potency than **11a** with IC_{50} values of $74 \mu M$

(doctanoylation) and $89 \mu M$ (demyrystoylation), compared to values of 150 and $120 \mu M$, respectively, for **11a**.¹⁵¹

Another class of inhibitors directly related to the SIRT6 enzymatic mechanism are N^ϵ -thioacyl lysine peptides, which cause a stall of the catalysis after the nucleophilic attack of the (thio)carbonyl group to the C1' of nicotinamide-bound ribose that happens in the first step of the catalytic mechanism.¹⁵² Early reports following the thioacyl peptide strategy let to N^ϵ -thioacyl lysine pentapeptides **13a** and **13b** (Figure 11, upper panel) showing IC_{50} values toward SIRT6 deacetylase activity of 78 and $47 \mu M$, respectively.¹⁵³ These data indicate that replacement of a His residue with an Ala residue improves inhibitor activity. Both compounds inhibit SIRT1/2 with higher potency compared to SIRT6. Indeed, they both abolish SIRT1/2 almost completely at a $200 \mu M$ concentration, while the inhibition of SIRT6 was 62%

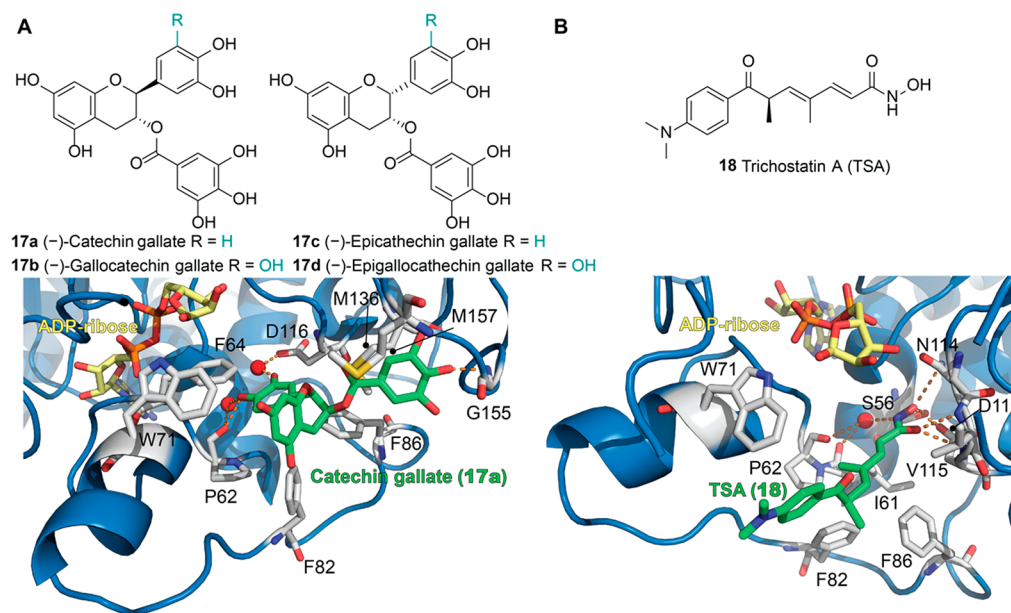


Figure 12. (A) Upper panel: Flavonole-based SIRT6 inhibitors. Lower panel: Structure of SIRT6 in complex with ADP-ribose (yellow) and catechin gallate (17a) (green) with a focus on the 17a binding site (PDB ID: 6QCJ). (B) Upper panel: TSA (18) structure. Lower panel: Structure of SIRT6 in complex with ADP-ribose (yellow) and 18 (green) with a focus on the 18 binding site (PDB ID: 6HOY). The binding mode is substantially different from 17a, although some interactions are shared, such as the key water-mediated hydrogen bond with Pro62 and the hydrophobic contacts with Trp71, Phe82, and Phe86. Key residues for compounds' binding are labeled, key water molecules for the protein-compound interaction are represented as red spheres, and polar interactions are shown as dashed orange lines.

(13a) and 91% (13b) at the same concentration. In the case of 13b, the IC_{50} values for SIRT1 and SIRT2 were 0.38 and 8.5 μM , respectively. These data are in line with the fact that both peptides are based on the sequence of p53, a known substrate of both SIRT1 and SIRT2. Nevertheless, although these molecules are not selective against SIRT6, they represent the first successful example of synthetic SIRT6 inhibitors.

A later study described the development of thiomristoyl peptides designed on the basis of SIRT6 natural substrates. In particular, compounds BHJH-TM1 (14a), BHJH-TM3 (14b), and BH-TM4 (14c) (Figure 11, middle panel) displayed SIRT6 inhibition in the low micromolar range with IC_{50} values for demyristoylation of 2.8, 8.1, and 1.7 μM , respectively.¹⁵⁴ These compounds were based on TNF α -K20, TNF α -K19, and H3K9 peptides, respectively. All three peptides were active against SIRT1/2/3, with IC_{50} values between 2.3 and 8.0 μM for all the isoforms, thus indicating a lack of selectivity and a mixed mode of action. Interestingly, they all displayed SIRT6 inhibition and increased TNF α fatty acylation in HEK293T cells with 14b being the most potent.

More recently, cyclic pentapeptides (15a–f) harboring a central N^{ϵ} -dodecyl- or N^{ϵ} -myristoyl-thiocarbamoyl-lysine (Figure 11, middle and lower panels) showed inhibitory activity toward SIRT6 in the nanomolar range (IC_{50} (15a) = 256 nM, IC_{50} (15b) = 282 nM, IC_{50} (15c) = 368 nM, IC_{50} (15d) = 319 nM, IC_{50} (15e) = 495 nM, IC_{50} (15f) = 319 nM). Compounds 15a–e had comparable IC_{50} values for SIRT1, while 15f an IC_{50} toward SIRT1 2.3 higher compared to SIRT6. Compounds 15e and 15f, bearing the same macrocycle bridging unit, were also tested against SIRT2 and SIRT3. Compound 15e showed moderate selectivity over SIRT2 and SIRT3 (~2.9-fold and ~1.5-fold, respectively), while 15f exhibited high selectivity over the two isoforms (20-fold and 11-fold, respectively). Finally, 15f was tested against SIRT5, where the results indicated that the molecule is substantially inactive towards this enzyme (IC_{50} >

300 μM). This analysis suggests that the only selective SIRT6 inhibitor is 15f.¹⁵⁵ Despite that, 15f was not able to inhibit SIRT6 inside the human pancreatic cancer BxPC3 cells, likely because of poor cellular permeability given its peptide nature and high molecular weight. Nonetheless, these peptides represent valuable lead compounds for the development of peptidomimetics inhibiting SIRT6.

Recently, Sociali et al. developed a lysine-based compound targeting SIRT6 deacetylase and deacylase activities (16, Figure 11, lower panel).¹⁵⁶ This molecule consists of a lysine residue whereby the N^{α} -amine group is protected with an acetyl group, while the carboxy group is coupled with a 12-carbon alkyl chain amine. This compound inhibited SIRT6 deacetylation (IC_{50} = 95 μM) without isoform specificity, as it inhibited also SIRT1 and SIRT2 with comparable potency (IC_{50} s = 51 and 102 μM , respectively). Remarkably, compound 16 behaved as a deacetylation activator showing 52% activation of demyristoylation (EC_{50} = 70 μM) and 80% activation of depalmitoylation at 100 μM while still acting as an inhibitor for SIRT1/2 deacetylation (IC_{50} (SIRT1) = 157 μM , IC_{50} (SIRT2) = 177 μM). 16 displayed competitive inhibition toward acetylated peptide, but not NAD^+ , and increased H3K9 acetylation in the MCF-7 breast cancer cell line. Moreover, the activities of key glycolysis enzymes were increased, in line with SIRT6 involvement in downregulation of glycolytic enzymes, and TNF- α secretion was reduced, consistently with the ability of SIRT6 to trigger TNF- α secretion.^{22,30} The results obtained in this study are rather surprising in light of the evidence reported by Feldman et al. that FFAs determine enhancement of deacetylation activity and inhibition of deacetylation.²⁰ Based on *in silico* data, the authors speculate that the acetyl moiety bound to the $C\alpha$ amine group may mimic the acetylated substrate, being close to NAD^+ , in agreement with the observed competition with acetylated substrate and not with NAD^+ . However, further experimental

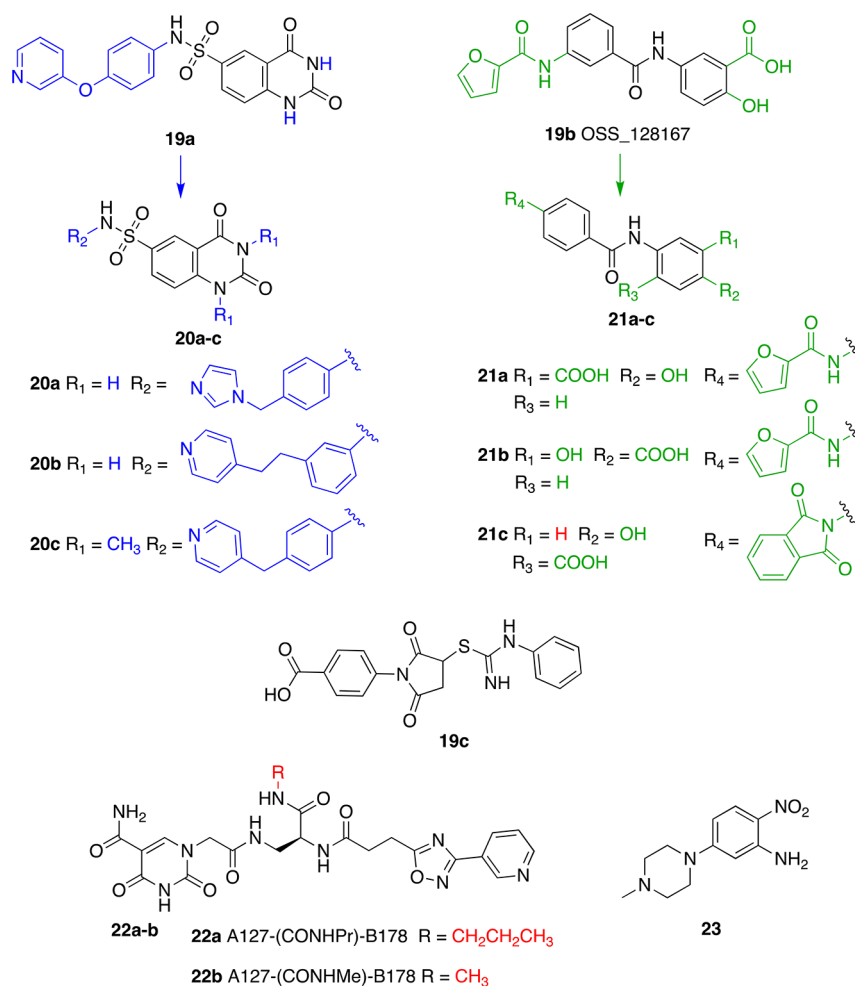


Figure 13. Synthetic small-molecule SIRT6 inhibitors.

evidence is necessary to clarify the binding mode and account for the differential SIRT6 modulation profile.

Interestingly, the **3b** derivatives (–)-catechin gallate (**17a**) and (–)-gallocatechin gallate (**17b**) displayed inhibition of SIRT6-mediated deacetylation in the low micromolar range (IC_{50} (**17a**) = 2.5 μ M; IC_{50} (**17b**) = 5.4 μ M).¹⁰³ The epimers of compounds **17a** and **17b**, (–)-epicatechin gallate (**17c**) and (–)-epigallocatechin gallate (**17d**), displayed lower activity toward SIRT6, with ~60 and ~40% inhibition at 100 μ M, respectively, compared to ~85–90% inhibition of **17a–b** at the same concentration. Structurally, these compounds differ from **3b** in ring C, which is reduced and presents a 3,4,5-trihydroxybenzoyl substitution. The **17a**–SIRT6 cocrystal (PDB ID: 6QCJ, Figure 12A) indicated that the inhibitor shares the same binding site as **3b** with identical conformations of the catechol groups, while the chromen-4-one of **17a** was rotated to accommodate the bulky trihydroxybenzoyl moiety. Ring C interacts with Trp71 of the acyl channel exit, and the trihydroxybenzoyl portion forms hydrophobic interactions with the other side of the channel and a hydrogen bond with the backbone of Gly155. It appears that the main difference between **3b**-derived activators and inhibitors consists of the presence of the bulky substituent on ring C and consequent tilted position of the chroman, which is saturated in inhibitors **17a,b**. This is supported by the fact that the orientation of the pyrrolo[1,2-*a*]quinoxaline of the SIRT6 activator **5** is similar to the ring C of **3b** derivatives, rather than **17a**. Nonetheless, these compounds

were not tested against other SIRT or HDAC isoforms, so their selectivity needs to be further investigated. In addition, given their polyphenolic structure, both compounds very likely display pleiotropic off-target effects, as previously described for compounds **3a–e**. Indeed, **17a–b** also inhibit α -glucosidase,¹⁵⁷ while inhibition of topoisomerases has been widely reported for the **17b** epimer **17d**.^{158,159} This compound also exhibited dual activity toward SIRT3, acting as either an activator or inhibitor depending on the cellular context.¹⁶⁰ In addition, **17d** inhibits DNMT1^{113,114} and different HAT enzymes such as p300, CBP, PCAF, and Tip60.^{86,87} Even though **17a–b** have poor specificity, the availability of the SIRT6–**17a** cocrystal structure could be exploited by medicinal chemists for drug design, as previously mentioned in the case of activators **3b** and **3e**.

Trichostatin A (**18**, TSA), a hydroxamate derivative known for its nanomolar inhibitory activity of class I and II HDACs given its zinc-chelating properties, was recently found to inhibit SIRT6.¹⁶¹ Though no IC_{50} was calculated, the K_i values for **18**-mediated SIRT6 deacetylation were 2.02 μ M when using H3K9Ac peptide and 4.62 μ M when using p53K382Ac peptide. No inhibitory activity was observed against SIRT1–3 and SIRT5 up to a 50 μ M concentration. Kinetic analysis indicated competitive inhibition toward the acetylated peptide but not NAD^+ . The crystal structure of the SIRT6/ADP–ribose/**18** complex (PDB ID: 6HOY, Figure 12B) indicated the binding of **18** to the acyl channel extension of SIRT6, explaining its isoform specificity.¹⁶² The hydroxamate moiety of **18** engages in polar

interactions, including a water-mediated hydrogen bond between **18** nitrogen and the backbone oxygens of Ile 61 and Pro62. The carbonyl group is involved in hydrogen bonds with the backbone nitrogen of Val115 and Asp116. In addition, the **18** hydroxyl moiety acts as a hydrogen bond donor in its interaction with the side chains of Asn114 and Asp116 (Figure 12B). The **18** hydroxamate group mimics **11a** interactions, as confirmed by a competition binding assay in the presence of **11a**. Since no **18**/NAD⁺ competition was observed in activity assays, the authors propose a mechanism whereby **18** interacts with the **11a** binding region following the release of the **11a** moiety from NAD⁺. They also argue that the reported acetylated peptide competition is caused indirectly, by inducing conformational changes leading to clashes with the acylated substrate.

Beyond drug repurposing, the first synthetic small-molecule compounds displaying SIRT6 inhibition were identified by Parenti et al. following an *in silico* screening.¹⁶³ This approach led to the discovery of the derivatives **19a–c** (Figure 13) possessing IC₅₀ values of 106, 89, and 181 μM, respectively. Among them, compounds **19b** (subsequently named OSS_128167) and **19c** displayed selectivity over SIRT1 and SIRT2 (IC₅₀ values 8.44 to 19.15 times higher), while **19a** was mildly selective over SIRT1 (IC₅₀ = 314 μM) but not over SIRT2 (IC₅₀ = 114 μM). The three compounds increased H3K9 acetylation in BxPC3 cells and induced GLUT1 upregulation and consequent augmented glucose uptake in L6 rat myoblasts and BxPC3 cells. This is consistent with reports indicating the role of SIRT6 in GLUT1 downregulation.⁵⁹ Furthermore, the compounds were able to reduce TNF-α secretion. This study shows that small-molecule-mediated SIRT6 inhibition mimics the effects of SIRT6 knockdown. When tested in a murine model of type 2 diabetes, **19a** improved glucose tolerance and reduced plasma levels of insulin, triglycerides, and cholesterol.¹⁶⁴ Remarkably, **19b** reduced the recruitment of SIRT6 to DNA-damage locations and sensitized primary MM cells, along with melphalan- and doxorubicin-resistant MM cell lines, to DNA-damaging chemotherapeutics.¹⁶⁵ Compound **19b** also decreased the viability of DLBCL cells, usually displaying SIRT6 overexpression, and inhibited their proliferation in a time- and dose-dependent fashion, through induction of apoptosis and cell cycle arrest at G2/M phase. When tested in a mouse xenograft model with human DLBCL cells, **19b** reduced tumor growth and decreased the levels of the proliferative marker Ki-67.⁷⁹ Nevertheless, these reports lack of target engagement studies demonstrating that **19b** does bind to SIRT6 at least in the cellular context. Hence, the observed *in vivo* phenotype may be a consequence of off-target effects, particularly considering the weak *in vitro* potency of **19b**. To shed light on this, cellular and *in vivo* target engagement studies should be performed.^{139–143} Moreover, the comparison between the phenotypes induced by **19b** treatment, by SIRT6 gene knockdown, and by a combination of the two should also be carried out to clarify the mechanism of action^{144,145} and unambiguously link the observed anticancer effects to SIRT6 inhibition.

Optimization of compound **19a** led to the quinazolinone derivatives **20a–c** (Figure 13, left).¹⁶⁶ Compounds **20a** and **20b** are characterized by different substituents on the sulphonamide residue; in addition to this, in compound **20c**, the nitrogen atoms of the quinazolinone core are methylated. These substitutions led to improved SIRT6 inhibition (IC₅₀ (**20a**) = 60 μM; IC₅₀ (**20b**) = 37 μM; IC₅₀ (**20c**) = 49 μM). Compound **20a** was slightly selective over SIRT1 and SIRT2 with IC₅₀ values of 238 and 159 μM, respectively. Compounds **20b–c** exhibited

good selectivity over SIRT1 (IC₅₀ values were 11 and 133 times higher, respectively) and low selectivity over SIRT2 (2.30-fold and 4.94-fold, respectively), although the activity against other isoforms remains to be tested. It appears that removal of oxygen in the sulphonamide side-chain and the extension of the aliphatic spacer between the aromatic groups (see **20b**) improves the inhibitory efficiency of these derivatives. In addition, the simultaneous oxygen removal from the side chain and methylation of the quinazolinone nitrogens increases isoform specificity. These derivatives increased H3K9 acetylation in BxPC3, but only compounds **20b** and **20c** caused increased glucose uptake in L6 rat myoblasts and BxPC3 cells. Remarkably, **20a** and **20b** were able to sensitize BxPC3 cells to the chemotherapeutic gemcitabine. Compound **20c** was not evaluated *in vivo*, since it was found to be cytotoxic at a concentration close to its IC₅₀ (30 μM). Compounds **19a** and **20b** were found to effectively enhance the anticancer activity of the PARP inhibitor olaparib in Capan-1 cells (a BRCA2-deficient pancreatic cancer cell line). These observations are consistent with previous findings suggesting that SIRT6 knockdown improves the efficacy of chemotherapeutics.¹⁶⁷

The salicylate derivative **19b** was further optimized yielding the highly selective SIRT6 inhibitors **21a–c** (Figure 13, right). Compound **21a** is an analogue of **19b**, in which the furan-2-carboxamide moiety is shifted from 3' to 4'. Compound **21b** presents the furan-2-carboxamide at the same position as **21a** but has the hydroxyl and carboxylic groups swapped with each other. **21a** and **21b** have IC₅₀ values of 34 and 22 μM, respectively. These data indicate that the presence of the furan-2-carboxamide at *para* position massively increases the SIRT6 inhibitory activity, while the swap of hydroxyl and carboxylic groups leads to only a slight improvement of the inhibition. In compound **21c**, a phthalimide moiety replaces the furan-2-carboxamide in 3', while the carboxylic and hydroxyl groups are in positions 2 and 4, respectively. These modifications furnished a compound with slightly improved inhibitory efficacy, having an IC₅₀ of 20 μM.¹⁶⁸ All compounds displayed selectivity over SIRT1 and SIRT2 (IC₅₀ values between 13 and 27 times higher), although the selectivity over other SIRT isoforms needs to be evaluated. Compounds **21a** and **21b** increased H3K9 acetylation and glucose uptake in human peripheral blood mononuclear cells (PBMCs), in line with previous studies and with the roles of SIRT6 in cell homeostasis. Conversely, compound **21c** did not show any effect in cell-based assays, probably due to a lack of cell permeability. Compounds **21a** and **21b** also impaired TNF-α secretion and sensitized pancreatic cancer cells to gemcitabine. Compound **21b** also presented antiproliferative properties in PBMCs.

Compound screening based on a DNA-encoded library designed for NAD⁺-binding pockets led to the identification of two SIRT6 inhibitors with a 5-aminocarbonyl-uracil core (Figure 13, lower panel): A127-(CONHPr)-B178 (**22a**) and A127-(CONHMe)-B178 (**22b**). Both molecules were evaluated in a demyristoylation assay and displayed IC₅₀ values of 6.7 and 9.2 μM, respectively.¹⁶⁹ Compound **22a** was selective over other SIRTs, as inhibition of SIRT1–3, SIRT5, and SIRT7 was less than 10% at 10 μM and was stable in serum after 72 h. It caused an increase of DNA-damage markers and telomere-dysfunction-induced *foci* in primary human umbilical venous endothelial cells (HUVECs), like what was observed following SIRT6 knockdown.¹⁷⁰ Similarly to other SIRT6 inhibitors, **22a** caused a dose-dependent decrease in the TNF-α levels.

Recently, a series of 1-phenylpiperazine derivatives have been reported as a SIRT6 inhibitors. Among them, 5-(4-methylpiperazin-1-yl)-2-nitroaniline (**23**, Figure 13, lower panel) displayed an IC_{50} of 4.93 μ M in a peptide deacetylation assay and showed no activity against SIRT1–3 and HDAC1–11 up to 200 μ M concentration.¹⁷¹ When tested in BxPC-3 cells, compound **23** augmented the level of both H3K9 and H3K18 acetylation in a dose-dependent manner and increased GLUT1 expression levels. In addition, it reduced the blood glucose content in a mouse model of type 2 diabetes, thus demonstrating promising lead-like properties.

CONCLUSIONS

Mounting evidence supports the critical roles of SIRT6 in multiple processes regulating both physiological and pathological states. Although SIRT6 shares mechanistic features with other SIRT6s, it differs from them, as it greatly depends on FFA activation to increase the efficiency of its enzymatic activities.^{20,22} Through its multiple enzymatic activities, SIRT6 finely regulates not only genome maintenance and DNA repair but also stem cell differentiation, metabolism, and aging. The involvement of SIRT6 in these key processes may explain its dual role in cancer. For instance, DNA repair promotion may help evasion from tumorigenic transformation at early phases of cancer. On the other hand, the same mechanism may facilitate cancer progression at later stages or decrease the effectiveness of cytotoxic drug chemotherapy. It is worth noticing that the upregulation of SIRT6 in certain types of cancers^{76–79} may be representative of a compensatory effect rather than the cause itself of tumor initiation and/or progression.⁷⁶

SIRT6 also regulates crucial proteins involved in sugar homeostasis, as it promotes the expression of glycolytic genes,^{59,60} suppressing gluconeogenesis and increasing insulin secretion, hence having a favorable role in diabetes. The downregulation of glycolytic genes also acts as a tumor-suppressor pathway, since it suppresses the Warburg effect.⁵⁸ SIRT6 also regulates fat metabolism by reducing LDL-cholesterol levels⁹⁵ and triglyceride synthesis as well as promoting fatty-acid β -oxidation,⁴⁷ being a key player in obesity prevention. Like the double-faced role in cancer, SIRT6 has contrasting actions in the regulation of inflammation.^{80,84,85}

Although the growing knowledge about SIRT6 biology has been uncovering multifaceted functions in human diseases, the discovery of potent and selective SIRT6 modulators is at its infancy. The notion that FFAs increase the deacetylation efficiency of SIRT6 led to the investigation and discovery of the first SIRT6 activators. Initial hit compounds were derived from simple modifications of fatty acids, such as the ethanolamides **2a** and **2b**.¹⁰² Subsequent synthetic activators overcame issues directly related to the lipidic structure, such as metabolic instability, poor cellular permeability, and low water solubility. Ligand-based drug design efforts led to **5**, the first synthetic activator yielding cellular effects at mid- μ M concentrations.^{124,125} This discovery paved the way for the development of further activators, such as **7a**.¹²⁸ Although the binding mode of the analogue **7b** raised some discussion,^{130,131} it is possible that both proposed models are valid in different conditions, and this controversy reminds us that ligand–protein interactions cannot be always recapitulated by a single-crystal structure. In any case, both **7a** and its derivative **7c**¹³² inhibited tumor growth in xenograft models, showing SIRT6 activation efficacy *in vivo* for the first time.^{129,132} The recently described activator **10b**,¹³⁸ developed using the **5** binding mode as a model, displayed

efficacy at low micromolar concentrations, being an activator of both deacetylation and demyristoylation activities. Remarkably, it also possessed antitumor activity *in vivo*, even though it showed poor water solubility and very low bioavailability. Notably, CETSA measurements demonstrated that **10b** binds to SIRT6 in cells. Nonetheless, further studies are necessary to verify whether the observed phenotypic effects are genuinely related only to SIRT6 activation. Anyhow, **10b** represents a good lead compound that still necessitates a full validation and optimization of the pharmacodynamic and pharmacokinetic properties to be considered as a therapeutic option in the PDAC context.

In the case of inhibitors, the development of substrate-based peptidomimetics led to compounds **15a–f** that displayed SIRT6 inhibition in the nanomolar range, although the only compound tested *in vivo* (**15f**) did not show any effect. Nonetheless, given the high potency, these compounds represent optimal starting scaffolds for further developments, first aimed at improving the cellular permeability. Differently, compounds **19b**, **20b**, and **21b**, developed following structure- and ligand-based drug design strategies, were cellularly active, although they inhibited SIRT6 enzymatic activity only in the micromolar range. **19b** also displayed efficacy in a mouse xenograft model of DLBCL; however, additional analyses are necessary to demonstrate a causal correlation between its anticancer activity and SIRT6 inhibition. Therefore, currently, **19b** can be considered only a hit molecule that needs complete validation and, in case, extensive optimization of potency and selectivity.

Innovative approaches relying on high-throughput compound testing hold great potential for drug discovery. Compound **22a** has been discovered by means of DNA-encoded libraries,¹⁶⁹ a combinatorial approach in which the structure of each molecule is encoded by a conjugated DNA identifier sequence.^{172,173} This method allows quick testing of millions of combinations of fragments using micrograms of protein, offering the exploration of a vast chemical space. The successful application of this approach to SIRT6 led to a low micromolar inhibitor (**22a**) endowed with cellular activity. The application of this technique also to SIRT6 activator discovery would be very interesting.

Finally, compound **23** represents an exciting prospect. It showed low micromolar activity *in vitro* and was able to cause blood glucose reduction in a mouse model of diabetes.¹⁷¹ Moreover, its simple structure is amenable of modifications that may lead to more potent derivatives upon a proper structural optimization.

Different challenges have been characterizing the path to the discovery of SIRT6 modulators. These include initial difficulties of properly separating activation and inhibition and the suboptimal efficacy of currently discovered modulators, as explained by the absence of nanomolar activators thus far.

The recent discoveries of *in vivo* active compounds (particularly **7c** and **10b**) bring good hopes for the development of further potent and selective SIRT6 activators. In the case of inhibitors, researchers managed to obtain nanomolar or low micromolar compounds such as **15f**, **22a**, and **23**, plus the mid micromolar inhibitor **19b**, which was active both in cell and *in vivo*, although its SIRT6 target engagement needs to be demonstrated. These molecules cover different chemical classes, ranging from peptidomimetics to small molecules, and some of them represent ideal hit/lead compounds for further development.

Anyway, additional efforts are necessary to improve the potency of the currently available SIRT6 modulators, since

usually only nanomolar compounds have concrete chances to progress to preclinical and clinical phases.

To this end, structure-based drug design approaches might be particularly beneficial. Indeed, the availability of the crystal structures of SIRT6 in complex with both activators and inhibitors of polyphenolic nature, such as **3b**, **3e**, and **17a**, enable the identification of key features for target recognition and activity modulation. These cocrystals could be exploited to develop new activating or inhibiting compounds whereby only the important hydroxyl groups are kept while removing the nonessential ones, thus abolishing their pleiotropic effects and increasing their specificity. Moreover, in order to increase potency and selectivity, scaffold hopping^{120,121} approaches could be applied to develop molecules bearing different core chemotypes but retaining the key moieties for SIRT6 interaction. The inspection of the X-ray solved crystal structures of SIRT6 in complex with different modulators that bind in the same pocket with similar binding modes such as the activators **3b** (Figure 6B) and **5** (Figure 7A) could be also leveraged for the structural optimization by combining crucial chemical features. For instance, compound **5** might be modified through the addition of polar groups to the pyridine moiety to form hydrogen bonds with the conserved water molecules bridging to Val115 and Asp116. Moreover, the addition of large hydrophobic groups to the benzene ring could allow further hydrophobic interactions to be established with the pocket formed by Ile61, Phe82 and Phe86.

In conclusion, the available cocrystal structures, along with cutting-edge approaches such as artificial-intelligence-driven drug design and DNA-encoded libraries, have great potential in allowing the evaluation of a more diverse chemical space to obtain molecules possessing drug-like properties to facilitate the discovery of new SIRT6 modulators. To date, the ideal scenario for the initial evaluation of SIRT6 targeting molecules relies on the integration of structural approaches with classic biophysical assays¹⁷⁴ and modern, label-free methods such as those based on mass spectrometry,^{175–177} to allow reliable assessment of protein–ligand interactions and avoid false positives and negatives that may impair the following steps of a drug discovery campaign.

AUTHOR INFORMATION

Corresponding Authors

Antonello Mai – Department of Drug Chemistry & Technologies, Sapienza University of Rome, 00185 Rome, Italy; orcid.org/0000-0001-9176-2382; Phone: +39 06 49913392; Email: antonello.mai@uniroma1.it; Fax: +39 06 49693268

Dante Rotili – Department of Drug Chemistry & Technologies, Sapienza University of Rome, 00185 Rome, Italy; orcid.org/0000-0002-8428-8763; Phone: +39 06 49913237; Email: dante.rotili@uniroma1.it; Fax: +39 06 49693268

Author

Francesco Fiorentino – Department of Chemistry, University of Oxford, Oxford OX1 3QZ, United Kingdom; orcid.org/0000-0003-3550-1860

Complete contact information is available at:
<https://pubs.acs.org/10.1021/acs.jmedchem.1c00601>

Author Contributions

The manuscript was written through contributions of all authors. All authors have given approval to the final version of the manuscript.

Notes

The authors declare no competing financial interest.

Biographies

Francesco Fiorentino graduated in Medicinal Chemistry at the University of Rome “La Sapienza” (Italy) in 2016. He received his Ph.D. in Biophysical Chemistry at University of Oxford (UK) in 2020 under the supervision of Prof. Dame Carol Robinson, working on the elucidation of the structure and regulation of membrane proteins using mass spectrometry. He is now a Postdoctoral Research Associate at the University of Oxford. His research activity has been directed toward the investigation of the molecular mechanisms underpinning protein function and modulation. To this end, he is applying native mass spectrometry and other biophysical techniques to investigate the protein complexes involved in bacterial membrane biogenesis and epigenetics.

Antonello Mai graduated in Pharmacy at the University of Rome “La Sapienza”, Italy, in 1984. He received his Ph.D. in 1992 in Pharmaceutical Sciences, with a thesis entitled “Researches on New Polycyclic Benzodiazepines Active on Central Nervous System”, with advisor Prof. M. Artico. In 1998, he was appointed Associate Professor of Medicinal Chemistry at the same University. In 2011, Prof. Mai was appointed Full Professor of Medicinal Chemistry at the Faculty of Pharmacy and Medicine, Sapienza University of Rome. He has published more than 250 papers in peer-reviewed high-impact factor journals. His research interests include the synthesis and biological evaluation of new bioactive small-molecule compounds, in particular modulators of epigenetic targets. In addition, he is working in the field of antibacterial/antimycobacterial, antiviral, and CNS agents.

Dante Rotili graduated in Medicinal Chemistry at the University of Rome “La Sapienza” (Italy) in 2003. He received his Ph.D. in Pharmaceutical Sciences at the same University in 2007. In 2009/2010, he was a research associate at the Department of Chemistry of the University of Oxford, where he worked in collaboration with Prof. C. Schofield in the development of chemoproteomic probes for the characterization of 2-oxoglutarate-dependent enzymes. In 2020, he was appointed as Associate Professor of Medicinal Chemistry at the University of Rome “La Sapienza”. Since 2017, he has had the Italian National Habilitation to Full Professor of Medicinal Chemistry. His research activity has been focusing mainly on the development of modulators of epigenetic enzymes with potential applications in cancer, neurodegenerative, metabolic, and infectious diseases.

ACKNOWLEDGMENTS

This work was supported by PRIN 2016 (prot. 20152TE5PK) (A.M.), AIRC 2016 (n. 19162) (A.M.), and Progetto di Ateneo “Sapienza” 2017 n. RM11715C7CA6CE53 (D.R.).

ABBREVIATIONS USED

5AC, 5-azacytidine; 5-hmC, 5-hydroxymethylcytosine; 5-mC, 5-methylcytosine; ABPP, affinity-based protein profiling; AMPK, AMP-activated protein kinase; Bax, Bcl-2-associated X protein; BER, base excision repair; CETSA, cellular thermal shift assay; CREB, cAMP response element-binding protein; CRC, colorectal cancer; DAC, decitabine; DDR, DNA-damage repair; DLBCL, diffuse large B-cell lymphoma; DNMT1, DNA methyltransferase 1; DSB, double-strand break; EMT, epithelial–mesenchymal transition; E2F1, E2 transcription factor 1;

FFA, free fatty acid; G6PC, glucose-6-phosphatase; FRET, fluorescence resonance energy transfer; GCNS, general control nonderepressible 5; GLUT, glucose transporter; HAT, histone acetyltransferase; HCC, hepatocellular carcinoma; HDASH, histone deacetylase assay homogeneous; HIF-1 α , hypoxia-inducible factor 1 α ; HR, homologous recombination; HSCs, hematopoietic stem cells; IGF, insulin-like growth factor; IGFBP, insulin-like growth factor-binding protein; IL-6, interleukin-6; IL-8, interleukin-8; iPSC, induced pluripotent stem cell; LDH, lactate dehydrogenase; LINE-1, long interspersed element-1; lncRNA, long noncoding RNA; MES, morpholinoethanesulfonic acid; MDM2, mouse double minute 2 homologue; MEFs, mouse embryonic fibroblasts; miRNA, micro-RNA; MM, multiple myeloma; MSCs, mesenchymal stem cells; NHEJ, nonhomologous end-joining; NPC, nasopharyngeal carcinoma; NRF2, nuclear factor erythroid 2-related factor; PAINS, pan assay interference compounds; PARP1, poly(ADP-ribose)polymerase 1; PBMC, peripheral blood mononuclear cell; PCPB2, poly(C)-binding protein 2; PCD, programmed cell death; PCK1, phosphoenolpyruvate carboxykinase; PCSK9, proprotein convertase subtilisin/kexin type 9; PDAC, pancreatic ductal adenocarcinoma; PDK1, pyruvate dehydrogenase kinase-1; PFK1, phosphofructokinase-1; PKM2, pyruvate kinase M2; PTM, post-translational modification; RTE, retrotransposable element; RUNX2, runt-related transcription factor 2; SIRT6, sirtuins; SIRT6, sirtuin 6; SUMO, small ubiquitin-related modifier; SREBP, sterol regulatory element-binding protein; TET, ten-11 translocation methylcytosine dioxygenase; TRF2, telomere repeat binding factor 2; TSA, trichostatin A; UTR, untranslated region; WRN, Werner syndrome ATP-dependent helicase; XIAP, X-linked inhibitor of apoptosis protein

REFERENCES

- (1) Finkel, T.; Deng, C. X.; Mostoslavsky, R. Recent progress in the biology and physiology of sirtuins. *Nature* **2009**, *460*, 587–591.
- (2) Chang, A. R.; Ferrer, C. M.; Mostoslavsky, R. SIRT6, a mammalian deacetylase with multitasking abilities. *Physiol. Rev.* **2020**, *100*, 145–169.
- (3) Klein, M. A.; Denu, J. M. Biological and catalytic functions of sirtuin 6 as targets for small-molecule modulators. *J. Biol. Chem.* **2020**, *295*, 11021–11041.
- (4) Liszt, G.; Ford, E.; Kurtev, M.; Guarente, L. Mouse Sir2 homologue SIRT6 is a nuclear ADP-ribosyltransferase. *J. Biol. Chem.* **2005**, *280*, 21313–21320.
- (5) Imai, S.-I.; Guarente, L. It takes two to tango: NAD(+) and sirtuins in aging/longevity control. *NPJ. Aging Mech. Dis.* **2016**, *2*, 16017.
- (6) Mostoslavsky, R.; Chua, K. F.; Lombard, D. B.; Pang, W. W.; Fischer, M. R.; Gellon, L.; Liu, P.; Mostoslavsky, G.; Franco, S.; Murphy, M. M.; Mills, K. D.; Patel, P.; Hsu, J. T.; Hong, A. L.; Ford, E.; Cheng, H. L.; Kennedy, C.; Nunez, N.; Bronson, R.; Frendewey, D.; Auerbach, W.; Valenzuela, D.; Karow, M.; Hottiger, M. O.; Hursting, S.; Barrett, J. C.; Guarente, L.; Mulligan, R.; Demple, B.; Yancopoulos, G. D.; Alt, F. W. Genomic instability and aging-like phenotype in the absence of mammalian SIRT6. *Cell* **2006**, *124*, 315–329.
- (7) Kanfi, Y.; Naiman, S.; Amir, G.; Peshiti, V.; Zinman, G.; Nahum, L.; Bar-Joseph, Z.; Cohen, H. Y. The sirtuin SIRT6 regulates lifespan in male mice. *Nature* **2012**, *483*, 218–221.
- (8) Sebastián, C.; Zwaans, B. M. M.; Silberman, D. M.; Gymrek, M.; Goren, A.; Zhong, L.; Ram, O.; Truelove, J.; Guimaraes, A. R.; Toiber, D.; Cosentino, C.; Greenon, J. K.; MacDonald, A. I.; McGlynn, L.; Maxwell, F.; Edwards, J.; Giacosa, S.; Guccione, E.; Weissleder, R.; Bernstein, B. E.; Regev, A.; Shiels, P. G.; Lombard, D. B.; Mostoslavsky, R. The histone deacetylase SIRT6 is a tumor suppressor that controls cancer metabolism. *Cell* **2012**, *151*, 1185–1199.
- (9) Kugel, S.; Feldman, J. L.; Klein, M. A.; Silberman, D. M.; Sebastián, C.; Mermel, C.; Dobersch, S.; Clark, A. R.; Getz, G.; Denu, J. M.; Mostoslavsky, R. Identification of and Molecular Basis for SIRT6 Loss-of-Function Point Mutations in Cancer. *Cell Rep.* **2015**, *13*, 479–488.
- (10) de Ceu Teixeira, M.; Sanchez-Lopez, E.; Espina, M.; Garcia, M. L.; Durazzo, A.; Lucarini, M.; Novellino, E.; Souto, S. B.; Santini, A.; Souto, E. B. Sirtuins and SIRT6 in Carcinogenesis and in Diet. *Int. J. Mol. Sci.* **2019**, *20*, 4945.
- (11) Fiorentino, F.; Carafa, V.; Favale, G.; Altucci, L.; Mai, A.; Rotili, D. The Two-Faced Role of SIRT6 in Cancer. *Cancers* **2021**, *13*, 1156.
- (12) Ferrer, C. M.; Alders, M.; Postma, A. V.; Park, S.; Klein, M. A.; Cetinbas, M.; Pajkrt, E.; Glas, A.; van Koningsbruggen, S.; Christoffels, V. M.; Mannens, M. M. A. M.; Knekt, L.; Etchegaray, J. P.; Sadreyev, R. I.; Denu, J. M.; Mostoslavsky, G.; van Maarle, M. C.; Mostoslavsky, R. An inactivating mutation in the histone deacetylase SIRT6 causes human perinatal lethality. *Genes Dev.* **2018**, *32*, 373–388.
- (13) Zhang, W.; Wan, H.; Feng, G.; Qu, J.; Wang, J.; Jing, Y.; Ren, R.; Liu, Z.; Zhang, L.; Chen, Z.; Wang, S.; Zhao, Y.; Wang, Z.; Yuan, Y.; Zhou, Q.; Li, W.; Liu, G. H.; Hu, B. SIRT6 deficiency results in developmental retardation in cynomolgus monkeys. *Nature* **2018**, *560*, 661–665.
- (14) Kanfi, Y.; Shalman, R.; Peshti, V.; Pilosof, S. N.; Gozlan, Y. M.; Pearson, K. J.; Lerrer, B.; Moazed, D.; Marine, J. C.; de Cabo, R.; Cohen, H. Y. Regulation of SIRT6 protein levels by nutrient availability. *FEBS Lett.* **2008**, *582*, 543–548.
- (15) Michishita, E.; McCord, R. A.; Berber, E.; Kioi, M.; Padilla-Nash, H.; Damian, M.; Cheung, P.; Kusumoto, R.; Kawahara, T. L. A.; Barrett, J. C.; Chang, H. Y.; Bohr, V. A.; Ried, T.; Gozani, O.; Chua, K. F. SIRT6 is a histone H3 lysine 9 deacetylase that modulates telomeric chromatin. *Nature* **2008**, *452*, 492–496.
- (16) Michishita, E.; McCord, R. A.; Boxer, L. D.; Barber, M. F.; Hong, T.; Gozani, O.; Chua, K. F. Cell cycle-dependent deacetylation of telomeric histone H3 lysine K56 by human SIRT6. *Cell Cycle* **2009**, *8*, 2664–2666.
- (17) Yang, B.; Zwaans, B. M. M.; Eckersdorff, M.; Lombard, D. B. The sirtuin SIRT6 deacetylates H3 K56Ac in vivo to promote genomic stability. *Cell Cycle* **2009**, *8*, 2662–2663.
- (18) Tasselli, L.; Xi, Y.; Zheng, W.; Tennen, R. I.; Odrowaz, Z.; Simeoni, F.; Li, W.; Chua, K. F. SIRT6 deacetylates H3K18ac at pericentric chromatin to prevent mitotic errors and cellular senescence. *Nat. Struct. Mol. Biol.* **2016**, *23*, 434–440.
- (19) Pan, P. W.; Feldman, J. L.; Devries, M. K.; Dong, A.; Edwards, A. M.; Denu, J. M. Structure and biochemical functions of SIRT6. *J. Biol. Chem.* **2011**, *286*, 14575–14587.
- (20) Feldman, J. L.; Baeza, J.; Denu, J. M. Activation of the protein deacetylase SIRT6 by long-chain fatty acids and widespread deacetylation by Mammalian Sirtuins. *J. Biol. Chem.* **2013**, *288*, 31350–31356.
- (21) Klein, M. A.; Liu, C.; Kuznetsov, V. I.; Feltenberger, J. B.; Tang, W.; Denu, J. M. Mechanism of activation for the sirtuin 6 protein deacetylase. *J. Biol. Chem.* **2020**, *295*, 1385–1399.
- (22) Jiang, H.; Khan, S.; Wang, Y.; Charron, G.; He, B.; Sebastian, C.; Du, J.; Kim, R.; Ge, E.; Mostoslavsky, R.; Hang, H. C.; Hao, Q.; Lin, H. SIRT6 regulates TNF- α secretion through hydrolysis of long-chain fatty acyl lysine. *Nature* **2013**, *496*, 110–113.
- (23) Zhang, X.; Spiegelman, N. A.; Nelson, O. D.; Jing, H.; Lin, H. SIRT6 regulates Ras-related protein R-Ras2 by lysine defatty-acylation. *eLife* **2017**, *6*, No. e25158.
- (24) Finin, M. S.; Donigian, J. R.; Pavletich, N. P. Structure of the histone deacetylase SIRT2. *Nat. Struct. Biol.* **2001**, *8*, 621–625.
- (25) Schuetz, A.; Min, J.; Antoshenko, T.; Wang, C. L.; Allali-Hassani, A.; Dong, A.; Loppnau, P.; Vedadi, M.; Bochkarev, A.; Sternglanz, R.; Plotnikov, A. N. Structural Basis of Inhibition of the Human NAD⁺-Dependent Deacetylase SIRT5 by Suramin. *Structure* **2007**, *15*, 377–389.
- (26) Jin, L.; Wei, W.; Jiang, Y.; Peng, H.; Cai, J.; Mao, C.; Dai, H.; Choy, W.; Bemis, J. E.; Jirousek, M. R.; Milne, J. C.; Westphal, C. H.; Perni, R. B. Crystal structures of human SIRT3 displaying substrate-induced conformational changes. *J. Biol. Chem.* **2009**, *284*, 24394–24405.

- (27) Sanders, B. D.; Jackson, B.; Marmorstein, R. Structural basis for sirtuin function: What we know and what we don't. *Biochim. Biophys. Acta, Proteins Proteomics* **2010**, *1804*, 1604–1616.
- (28) Gil, R.; Barth, S.; Kanfi, Y.; Cohen, H. Y. SIRT6 exhibits nucleosome-dependent deacetylase activity. *Nucleic Acids Res.* **2013**, *41*, 8537–8545.
- (29) Wang, W. W.; Zeng, Y.; Wu, B.; Deiters, A.; Liu, W. R. A Chemical Biology Approach to Reveal Sirt6-targeted Histone H3 Sites in Nucleosomes. *ACS Chem. Biol.* **2016**, *11*, 1973–1981.
- (30) Zhang, X.; Khan, S.; Jiang, H.; Antonyak, M. A.; Chen, X.; Spiegelman, N. A.; Shrimp, J. H.; Cerione, R. A.; Lin, H. Identifying the functional contribution of the defatty-Acylase activity of SIRT6. *Nat. Chem. Biol.* **2016**, *12*, 614–620.
- (31) Van Meter, M.; Simon, M.; Tomblin, G.; May, A.; Morello, T. D.; Hubbard, B. P.; Bredbenner, K.; Park, R.; Sinclair, D. A.; Bohr, V. A.; Gorbunova, V.; Seluanov, A. JNK Phosphorylates SIRT6 to Stimulate DNA Double-Strand Break Repair in Response to Oxidative Stress by Recruiting PARP1 to DNA Breaks. *Cell Rep.* **2016**, *16*, 2641–2650.
- (32) Van Meter, M.; Kashyap, M.; Rezazadeh, S.; Geneva, A. J.; Morello, T. D.; Seluanov, A.; Gorbunova, V. SIRT6 represses LINE1 retrotransposons by ribosylating KAP1 but this repression fails with stress and age. *Nat. Commun.* **2014**, *5*, 5011.
- (33) Rezazadeh, S.; Yang, D.; Tomblin, G.; Simon, M.; Regan, S. P.; Seluanov, A.; Gorbunova, V. SIRT6 promotes transcription of a subset of NRF2 targets by mono-ADP-ribosylating BAF170. *Nucleic Acids Res.* **2019**, *47*, 7914–7928.
- (34) Rezazadeh, S.; Yang, D.; Biashad, S. A.; Firsanov, D.; Takasugi, M.; Gilbert, M.; Tomblin, G.; Bhanu, N. V.; Garcia, B. A.; Seluanov, A.; Gorbunova, V. SIRT6 mono-ADP ribosylates KDM2A to locally increase H3K36me2 at DNA damage sites to inhibit transcription and promote repair. *Aging* **2020**, *12*, 11165–11184.
- (35) Mostoslavsky, R.; Chua, K. F.; Lombard, D. B.; Pang, W. W.; Fischer, M. R.; Gellon, L.; Liu, P. F.; Mostoslavsky, G.; Franco, S.; Murphy, M. M.; Mills, K. D.; Patel, P.; Hsu, J. T.; Hong, A. L.; Ford, E.; Cheng, H. L.; Kennedy, C.; Nunez, N.; Bronson, R.; Frendewey, D.; Auerbach, W.; Valenzuela, D.; Karow, M.; Hottiger, M. O.; Hursting, S.; Barrett, J. C.; Guarente, L.; Mulligan, R.; Demple, B.; Yancopoulos, G. D.; Alt, F. W. Genomic instability and aging-like phenotype in the absence of mammalian SIRT6. *Cell* **2006**, *124*, 315–329.
- (36) McCord, R. A.; Michishita, E.; Hong, T.; Berber, E.; Boxer, L. D.; Kusumoto, R.; Guan, S.; Shi, X.; Gozani, O.; Burlingame, A. L.; Bohr, V. A.; Chua, K. F. SIRT6 stabilizes DNA-dependent protein kinase at chromatin for DNA double-strand break repair. *Aging* **2009**, *1*, 109–121.
- (37) Toiber, D.; Erdel, F.; Bouazoune, K.; Silberman, D.; Zhong, L.; Mulligan, P.; Sebastian, C.; Cosentino, C.; Martinez-Pastor, B.; Giacosa, S.; D'Urso, A.; Näär, A.; Kingston, R.; Rippe, K.; Mostoslavsky, R. SIRT6 recruits SNF2H to DNA break sites, preventing genomic instability through chromatin remodeling. *Mol. Cell* **2013**, *51*, 454–468.
- (38) Mao, Z.; Hine, C.; Tian, X.; Van Meter, M.; Au, M.; Vaidya, A.; Seluanov, A.; Gorbunova, V. SIRT6 promotes DNA repair under stress by activating PARP1. *Science* **2011**, *332*, 1443–1446.
- (39) Feldman, J. L.; Dittenhafer-Reed, K. E.; Kudo, N.; Thelen, J. N.; Ito, A.; Yoshida, M.; Denu, J. M. Kinetic and structural basis for Acyl-group selectivity and NAD⁺ dependence in sirtuin-catalyzed deacylation. *Biochemistry* **2015**, *54*, 3037–3050.
- (40) Onn, L.; Portillo, M.; Ilic, S.; Cleitman, G.; Stein, D.; Kaluski, S.; Shirat, I.; Slobodnik, Z.; Einav, M.; Erdel, F.; Akabayov, B.; Toiber, D. SIRT6 is a DNA double-strand break sensor. *eLife* **2020**, *9*, No. e51636.
- (41) Kaluski, S.; Portillo, M.; Besnard, A.; Stein, D.; Einav, M.; Zhong, L.; Ueberham, U.; Arendt, T.; Mostoslavsky, R.; Sahay, A.; Toiber, D. Neuroprotective Functions for the Histone Deacetylase SIRT6. *Cell Rep.* **2017**, *18*, 3052–3062.
- (42) Xu, Z.; Zhang, L.; Zhang, W.; Meng, D.; Zhang, H.; Jiang, Y.; Xu, X.; Van Meter, M.; Seluanov, A.; Gorbunova, V.; Mao, Z. SIRT6 rescues the age related decline in base excision repair in a PARP1-dependent manner. *Cell Cycle* **2015**, *14*, 269–276.
- (43) Hwang, B. J.; Jin, J.; Gao, Y.; Shi, G.; Madabushi, A.; Yan, A.; Guan, X.; Zalzman, M.; Nakajima, S.; Lan, L.; Lu, A. L. SIRT6 protein deacetylase interacts with MYH DNA glycosylase, APE1 endonuclease, and Rad9-Rad1-Hus1 checkpoint clamp. *BMC Mol. Biol.* **2015**, *16*, 12.
- (44) Rizzo, A.; Iachettini, S.; Salvati, E.; Zizza, P.; Maresca, C.; D'Angelo, C.; Benarroch-Popivker, D.; Capolupo, A.; Del Gaudio, F.; Cosconati, S.; Di Maro, S.; Merlino, F.; Novellino, E.; Amoreo, C. A.; Mottolose, M.; Sperduti, I.; Gilson, E.; Biroccio, A. SIRT6 interacts with TRF2 and promotes its degradation in response to DNA damage. *Nucleic Acids Res.* **2017**, *45*, 1820–1834.
- (45) Kawahara, T. L. A.; Michishita, E.; Adler, A. S.; Damian, M.; Berber, E.; Lin, M.; McCord, R. A.; Ongaiqui, K. C. L.; Boxer, L. D.; Chang, H. Y.; Chua, K. F. SIRT6 Links Histone H3 Lysine 9 Deacetylation to NF- κ B-Dependent Gene Expression and Organismal Life Span. *Cell* **2009**, *136*, 62–74.
- (46) Etchegaray, J. P.; Chavez, L.; Huang, Y.; Ross, K. N.; Choi, J.; Martinez-Pastor, B.; Walsh, R. M.; Sommer, C. A.; Lienhard, M.; Gladden, A.; Kugel, S.; Silberman, D. M.; Ramaswamy, S.; Mostoslavsky, G.; Hochedlinger, K.; Goren, A.; Rao, A.; Mostoslavsky, R. The histone deacetylase SIRT6 controls embryonic stem cell fate via TET-mediated production of 5-hydroxymethylcytosine. *Nat. Cell Biol.* **2015**, *17*, S45–S57.
- (47) Kim, H. S.; Xiao, C.; Wang, R. H.; Lahusen, T.; Xu, X.; Vassilopoulos, A.; Vazquez-Ortiz, G.; Jeong, W. I.; Park, O.; Ki, S. H.; Gao, B.; Deng, C. X. Hepatic-specific disruption of SIRT6 in mice results in fatty liver formation due to enhanced glycolysis and triglyceride synthesis. *Cell Metab.* **2010**, *12*, 224–236.
- (48) Kemp, J. R.; Longworth, M. S. Crossing the LINE toward genomic instability: LINE-1 retrotransposition in cancer. *Front. Chem.* **2015**, *3*, 68.
- (49) Tan, Y.; Xue, Y.; Song, C.; Grunstein, M. Acetylated histone H3K56 interacts with Oct4 to promote mouse embryonic stem cell pluripotency. *Proc. Natl. Acad. Sci. U. S. A.* **2013**, *110*, 11493–11498.
- (50) Xie, W.; Song, C.; Young, N. L.; Sperling, A. S.; Xu, F.; Sridharan, R.; Conway, A. E.; Garcia, B. A.; Plath, K.; Clark, A. T.; Grunstein, M. Histone H3 Lysine 56 Acetylation Is Linked to the Core Transcriptional Network in Human Embryonic Stem Cells. *Mol. Cell* **2009**, *33*, 417–427.
- (51) Koh, K. P.; Yabuuchi, A.; Rao, S.; Huang, Y.; Cunniff, K.; Nardone, J.; Laiho, A.; Tahiliani, M.; Sommer, C. A.; Mostoslavsky, G.; Lahesmaa, R.; Orkin, S. H.; Rodig, S. J.; Daley, G. Q.; Rao, A. Tet1 and Tet2 regulate 5-hydroxymethylcytosine production and cell lineage specification in mouse embryonic stem cells. *Cell Stem Cell* **2011**, *8*, 200–213.
- (52) Pan, H.; Guan, D.; Liu, X.; Li, J.; Wang, L.; Wu, J.; Zhou, J.; Zhang, W.; Ren, R.; Zhang, W.; Li, Y.; Yang, J.; Hao, Y.; Yuan, T.; Yuan, G.; Wang, H.; Ju, Z.; Mao, Z.; Li, J.; Qu, J.; Tang, F.; Liu, G. H. SIRT6 safeguards human mesenchymal stem cells from oxidative stress by coactivating NRF2. *Cell Res.* **2016**, *26*, 190–205.
- (53) Sun, H.; Wu, Y.; Fu, D.; Liu, Y.; Huang, C. SIRT6 regulates osteogenic differentiation of rat bone marrow mesenchymal stem cells partially via suppressing the nuclear factor- κ B signaling pathway. *Stem Cells* **2014**, *32*, 1943–1955.
- (54) Wang, H.; Diao, D.; Shi, Z.; Zhu, X.; Gao, Y.; Gao, S.; Liu, X.; Wu, Y.; Rudolph, K. L.; Liu, G.; Li, T.; Ju, Z. SIRT6 Controls Hematopoietic Stem Cell Homeostasis through Epigenetic Regulation of Wnt Signaling. *Cell Stem Cell* **2016**, *18*, 495–507.
- (55) Sharma, A.; Diecke, S.; Zhang, W. Y.; Lan, F.; He, C.; Mordwinkin, N. M.; Chua, K. F.; Wu, J. C. The role of SIRT6 protein in aging and reprogramming of human induced pluripotent stem cells. *J. Biol. Chem.* **2013**, *288*, 18439–18447.
- (56) Zhao, G.; Wang, H.; Xu, C.; Wang, P.; Chen, J.; Wang, P.; Sun, Z.; Su, Y.; Wang, Z.; Han, L.; Tong, T. SIRT6 delays cellular senescence by promoting p27Kip1 ubiquitin-proteasome degradation. *Aging* **2016**, *8*, 2308–2323.
- (57) Zhang, N.; Li, Z.; Mu, W.; Li, L.; Liang, Y.; Lu, M.; Wang, Z.; Qiu, Y.; Wang, Z. Calorie restriction-induced SIRT6 activation delays aging by suppressing NF- κ B signaling. *Cell Cycle* **2016**, *15*, 1009–1018.

- (58) Warburg, O. On the origin of cancer cells. *Science* **1956**, *123*, 309–314.
- (59) Zhong, L.; D'Urso, A.; Toiber, D.; Sebastian, C.; Henry, R. E.; Vadysirisack, D. D.; Guimaraes, A.; Marinelli, B.; Wikstrom, J. D.; Nir, T.; Clish, C. B.; Vaitheesvaran, B.; Iliopoulos, O.; Kurland, I.; Dor, Y.; Weissleder, R.; Shirihai, O. S.; Ellisen, L. W.; Espinosa, J. M.; Mostoslavsky, R. The Histone Deacetylase Sirt6 Regulates Glucose Homeostasis via Hif1 α . *Cell* **2010**, *140*, 280–293.
- (60) Bhardwaj, A.; Das, S. SIRT6 deacetylates PKM2 to suppress its nuclear localization and oncogenic functions. *Proc. Natl. Acad. Sci. U. S. A.* **2016**, *113*, E538–E547.
- (61) Wu, M.; Seto, E.; Zhang, J. E2F1 enhances glycolysis through suppressing Sirt6 transcription in cancer cells. *Oncotarget* **2015**, *6*, 11252–11263.
- (62) Choe, M.; Brusgard, J. L.; Chumsri, S.; Bhandary, L.; Zhao, X. F.; Lu, S.; Goloubeva, O. G.; Polster, B. M.; Fiskum, G. M.; Girmun, G. D.; Kim, M. S.; Passaniti, A. The RUNX2 Transcription Factor Negatively Regulates SIRT6 Expression to Alter Glucose Metabolism in Breast Cancer Cells. *J. Cell. Biochem.* **2015**, *116*, 2210–2226.
- (63) Sah, N. K.; Khan, Z.; Khan, G. J.; Bisen, P. S. Structural, functional and therapeutic biology of survivin. *Cancer Lett.* **2006**, *244*, 164–171.
- (64) Lin, X.; Shen, J.; Peng, D.; He, X.; Xu, C.; Chen, X.; Tanyi, J. L.; Montone, K.; Fan, Y.; Huang, Q.; Zhang, L.; Zhong, X. RNA-binding protein LIN28B inhibits apoptosis through regulation of the AKT2/FOXO3A/BIM axis in ovarian cancer cells. *Signal Transduct. Target. Ther.* **2018**, *3*, 23.
- (65) Min, L.; Ji, Y.; Bakiri, L.; Qiu, Z.; Cen, J.; Chen, X.; Chen, L.; Scheuch, H.; Zheng, H.; Qin, L.; Zatloukal, K.; Hui, L.; Wagner, E. F. Liver cancer initiation is controlled by AP-1 through SIRT6-dependent inhibition of survivin. *Nat. Cell Biol.* **2012**, *14*, 1203–1211.
- (66) Xia, Y.; Shen, S.; Verma, I. M. NF- κ B, an active player in human cancers. *Cancer Immunol. Res.* **2014**, *2*, 823–830.
- (67) Ouyang, L.; Yi, L.; Li, J.; Yi, S.; Li, S.; Liu, P.; Yang, X. SIRT6 overexpression induces apoptosis of nasopharyngeal carcinoma by inhibiting NF- κ B signaling. *OncoTargets Ther.* **2018**, *11*, 7613–7624.
- (68) Kugel, S.; Sebastián, C.; Fitamant, J.; Ross, K. N.; Saha, S. K.; Jain, E.; Gladden, A.; Arora, K. S.; Kato, Y.; Rivera, M. N.; Ramaswamy, S.; Sadreyev, R. I.; Goren, A.; Deshpande, V.; Bardeesy, N.; Mostoslavsky, R. SIRT6 suppresses pancreatic cancer through control of Lin28b. *Cell* **2016**, *165*, 1401–1415.
- (69) Cai, J.; Zuo, Y.; Wang, T.; Cao, Y.; Cai, R.; Chen, F. L.; Cheng, J.; Mu, J. A crucial role of SUMOylation in modulating Sirt6 deacetylation of H3 at lysine 56 and its tumor suppressive activity. *Oncogene* **2016**, *35*, 4949–4956.
- (70) Lin, Z.; Yang, H.; Tan, C.; Li, J.; Liu, Z.; Quan, Q.; Kong, S.; Ye, J.; Gao, B.; Fang, D. USP10 Antagonizes c-Myc transcriptional activation through SIRT6 stabilization to suppress tumor formation. *Cell Rep.* **2013**, *5*, 1639–1649.
- (71) Lee, N.; Ryu, H. G.; Kwon, J. H.; Kim, D. K.; Kim, S. R.; Wang, H. J.; Kim, K. T.; Choi, K. Y. SIRT6 depletion suppresses tumor growth by promoting cellular senescence induced by DNA damage in HCC. *PLoS One* **2016**, *11*, e0165835.
- (72) Feng, X. X.; Luo, J.; Liu, M.; Yan, W.; Zhou, Z. Z.; Xia, Y. J.; Tu, W.; Li, P. Y.; Feng, Z. H.; Tian, D. A. Sirtuin 6 promotes transforming growth factor- β 1/H2O2/HOCl-mediated enhancement of hepatocellular carcinoma cell tumorigenicity by suppressing cellular senescence. *Cancer Sci.* **2015**, *106*, 559–566.
- (73) Ran, L. K.; Chen, Y.; Zhang, Z. Z.; Tao, N. N.; Ren, J. H.; Zhou, L.; Tang, H.; Chen, X.; Chen, K.; Li, W. Y.; Huang, A. L.; Chen, J. SIRT6 overexpression potentiates apoptosis evasion in hepatocellular carcinoma via BCL2-associated X protein-dependent apoptotic pathway. *Clin. Cancer Res.* **2016**, *22*, 3372–3382.
- (74) Han, L. L.; Jia, L.; Wu, F.; Huang, C. Sirtuin6 (SIRT6) Promotes the EMT of Hepatocellular Carcinoma by Stimulating Autophagic Degradation of E-Cadherin. *Mol. Cancer Res.* **2019**, *17*, 2267–2280.
- (75) Zhang, Z.-G.; Qin, C.-Y. Sirt6 suppresses hepatocellular carcinoma cell growth via inhibiting the extracellular signal-regulated kinase signaling pathway. *Mol. Med. Rep.* **2014**, *9*, 882–888.
- (76) Cea, M.; Cagnetta, A.; Adamia, S.; Acharya, C.; Tai, Y. T.; Fulciniti, M.; Ohguchi, H.; Munshi, A.; Acharya, P.; Bhasin, M. K.; Zhong, L.; Carrasco, R.; Monacelli, F.; Ballestrero, A.; Richardson, P.; Gobbi, M.; Lemoli, R. M.; Munshi, N.; Hideshima, T.; Nencioni, A.; Chauhan, D.; Anderson, K. C. Evidence for a role of the histone deacetylase SIRT6 in DNA damage response of multiple myeloma cells. *Blood* **2016**, *127*, 1138–1150.
- (77) Cagnetta, A.; Soncini, D.; Orecchioni, S.; Talarico, G.; Minetto, P.; Guolo, F.; Retali, V.; Colombo, N.; Carminati, E.; Clavio, M.; Miglino, M.; Bergamaschi, M.; Nahimana, A.; Duchosal, M.; Todoerti, K.; Neri, A.; Passalacqua, M.; Bruzzzone, S.; Nencioni, A.; Bertolini, F.; Gobbi, M.; Lemoli, R. M.; Cea, M. Depletion of SIRT6 enzymatic activity increases acute myeloid leukemia cells' vulnerability to DNA-damaging agents. *Haematologica* **2018**, *103*, 80–90.
- (78) Wang, J. C.; Kafeel, M. I.; Avezbakiyev, B.; Chen, C.; Sun, Y.; Rathnasabapathy, C.; Kalavar, M.; He, Z.; Burton, J.; Lichter, S. Histone Deacetylase in Chronic Lymphocytic Leukemia. *Oncology* **2011**, *81*, 325–329.
- (79) Yang, J.; Li, Y.; Zhang, Y.; Fang, X.; Chen, N.; Zhou, X.; Wang, X. Sirt6 promotes tumorigenesis and drug resistance of diffuse large B-cell lymphoma by mediating PI3K/Akt signaling. *J. Exp. Clin. Cancer Res.* **2020**, *39*, 142.
- (80) Bauer, I.; Grozio, A.; Lasiglie, D.; Basile, G.; Sturla, L.; Magnone, M.; Sociali, G.; Soncini, D.; Caffa, I.; Poggi, A.; Zoppoli, G.; Cea, M.; Feldmann, G.; Mostoslavsky, R.; Ballestrero, A.; Patrone, F.; Bruzzzone, S.; Nencioni, A. The NAD⁺-dependent histone deacetylase SIRT6 promotes cytokine production and migration in pancreatic cancer cells by regulating Ca²⁺ responses. *J. Biol. Chem.* **2012**, *287*, 40924–40937.
- (81) Krishnamoorthy, V.; Vilwanathan, R. Silencing Sirtuin 6 induces cell cycle arrest and apoptosis in non-small cell lung cancer cell lines. *Genomics* **2020**, *112*, 3703–3712.
- (82) Han, Z.; Liu, L.; Liu, Y.; Li, S. Sirtuin SIRT6 suppresses cell proliferation through inhibition of Twist1 expression in non-small cell lung cancer. *Int. J. Clin. Exp. Pathol.* **2014**, *7*, 4774–4781.
- (83) Van Gool, F.; Gallí, M.; Gueydan, C.; Kruys, V.; Prevot, P. P.; Bedalov, A.; Mostoslavsky, R.; Alt, F. W.; De Smedt, T.; Leo, O. Intracellular NAD levels regulate tumor necrosis factor protein synthesis in a sirtuin-dependent manner. *Nat. Med.* **2009**, *15*, 206–210.
- (84) Lee, Y.; Ka, S. O.; Cha, H. N.; Chae, Y. N.; Kim, M. K.; Park, S. Y.; Bae, E. J.; Park, B. H. Myeloid sirtuin 6 deficiency causes insulin resistance in high-fat diet-fed mice by eliciting macrophage polarization toward an M1 phenotype. *Diabetes* **2017**, *66*, 2659–2668.
- (85) Xiao, C.; Wang, R. H.; Lahusen, T. J.; Park, O.; Bertola, A.; Maruyama, T.; Reynolds, D.; Chen, Q.; Xu, X.; Young, H. A.; Chen, W. J.; Gao, B.; Deng, C. X. Progression of chronic liver inflammation and fibrosis driven by activation of c-JUN signaling in Sirt6 mutant mice. *J. Biol. Chem.* **2012**, *287*, 41903–41913.
- (86) Fiorentino, F.; Mai, A.; Rotili, D. Lysine acetyltransferase inhibitors: structure-activity relationships and potential therapeutic implications. *Future Med. Chem.* **2018**, *10*, 1067–1091.
- (87) Fiorentino, F.; Mai, A.; Rotili, D. Lysine Acetyltransferase Inhibitors From Natural Sources. *Front. Pharmacol.* **2020**, *11*, 1243.
- (88) Fiorentino, F.; Mai, A.; Rotili, D. HAT inhibitors in cancer therapy. *Histone Modifications in Therapy* **2020**, *20*, 51–80.
- (89) Dominy, J. E., Jr.; Lee, Y.; Jedrychowski, M. P.; Chim, H.; Jurczak, M. J.; Camporez, J. P.; Ruan, H. B.; Feldman, J.; Pierce, K.; Mostoslavsky, R.; Denu, J. M.; Clish, C. B.; Yang, X.; Shulman, G. I.; Gygi, S. P.; Puigserver, P. The Deacetylase Sirt6 Activates the Acetyltransferase GCN5 and Suppresses Hepatic Gluconeogenesis. *Mol. Cell* **2012**, *48*, 900–913.
- (90) Puigserver, P.; Rhee, J.; Donovan, J.; Walkey, C. J.; Yoon, J. C.; Oriente, F.; Kitamura, Y.; Altomonte, J.; Dong, H. J.; Accili, D.; Spiegelman, B. M. Insulin-regulated hepatic gluconeogenesis through FOXO1-PGC-1 α interaction. *Nature* **2003**, *423*, 550–555.

- (91) Schilling, M. M.; Oeser, J. K.; Boustead, J. N.; Flemming, B. P.; O'Brien, R. M. Gluconeogenesis: Re-evaluating the FOXO1-PGC-1 α connection. *Nature* **2006**, *443*, E10–E11.
- (92) Zhang, P.; Tu, B.; Wang, H.; Cao, Z.; Tang, M.; Zhang, C.; Gu, B.; Li, Z.; Wang, L.; Yang, Y.; Zhao, Y.; Wang, H.; Luo, J.; Deng, C. X.; Gao, B.; Roeder, R. G.; Zhu, W. G. Tumor suppressor p53 cooperates with SIRT6 to regulate gluconeogenesis by promoting FoxO1 nuclear exclusion. *Proc. Natl. Acad. Sci. U. S. A.* **2014**, *111*, 10684–10689.
- (93) Xiao, C.; Kim, H. S.; Lahusen, T.; Wang, R. H.; Xu, X.; Gavrilo, O.; Jou, W.; Gius, D.; Deng, C. X. SIRT6 deficiency results in severe hypoglycemia by enhancing both basal and insulin-stimulated glucose uptake in mice. *J. Biol. Chem.* **2010**, *285*, 36776–36784.
- (94) Chang, L.; Chiang, S. H.; Saltiel, A. R. Insulin signaling and the regulation of glucose transport. *Mol. Med.* **2004**, *10*, 65–71.
- (95) Kanfi, Y.; Peshti, V.; Gil, R.; Naiman, S.; Nahum, L.; Levin, E.; Kronfeld-Schor, N.; Cohen, H. Y. SIRT6 protects against pathological damage caused by diet-induced obesity. *Aging Cell* **2010**, *9*, 162–173.
- (96) Naiman, S.; Huynh, F. K.; Gil, R.; Glick, Y.; Shahar, Y.; Touitou, N.; Nahum, L.; Avivi, M. Y.; Roichman, A.; Kanfi, Y.; Gertler, A. A.; Doniger, T.; Ilkayeva, O. R.; Abramovich, I.; Yaron, O.; Lerrer, B.; Gottlieb, E.; Harris, R. A.; Gerber, D.; Hirschey, M. D.; Cohen, H. Y. SIRT6 Promotes Hepatic Beta-Oxidation via Activation of PPAR alpha. *Cell Rep.* **2019**, *29*, 4127–4143.
- (97) Abifadel, M.; Varret, M.; Rabès, J. P.; Allard, D.; Ouguerram, K.; Devillers, M.; Cruaud, C.; Benjannet, S.; Wickham, L.; Erlich, D.; Derré, A.; Villéger, L.; Farnier, M.; Beucler, I.; Bruckert, E.; Chambaz, J.; Chanu, B.; Lecerf, J. M.; Luc, G.; Moulin, P.; Weissenbach, J.; Prat, A.; Krempf, M.; Junien, C.; Seidah, N. G.; Boileau, C. Mutations in PCSK9 cause autosomal dominant hypercholesterolemia. *Nat. Genet.* **2003**, *34*, 154–156.
- (98) Tao, R.; Xiong, X.; DePinho, R. A.; Deng, C. X.; Dong, X. C. FoxO3 transcription factor and Sirt6 deacetylase regulate low density lipoprotein (LDL)-cholesterol homeostasis via control of the proprotein convertase subtilisin/kexin type 9 (Pcsk9) gene expression. *J. Biol. Chem.* **2013**, *288*, 29252–29259.
- (99) Tao, R.; Xiong, X.; DePinho, R. A.; Deng, C. X.; Dong, X. C. Hepatic SREBP-2 and cholesterol biosynthesis are regulated by FoxO3 and Sirt6. *J. Lipid Res.* **2013**, *54*, 2745–2753.
- (100) Elhanati, S.; Kanfi, Y.; Varvak, A.; Roichman, A.; Carmel-Gross, I.; Barth, S.; Gibor, G.; Cohen, H. Multiple regulatory layers of SREBP1/2 by SIRT6. *Cell Rep.* **2013**, *4*, 905–912.
- (101) Elhanati, S.; Ben-Hamo, R.; Kanfi, Y.; Varvak, A.; Glazz, R.; Lerrer, B.; Efroni, S.; Cohen, H. Y. Reciprocal Regulation between SIRT6 and miR-122 Controls Liver Metabolism and Predicts Hepatocarcinoma Prognosis. *Cell Rep.* **2016**, *14*, 234–242.
- (102) Rahnasto-Rilla, M.; Kokkola, T.; Jarho, E.; Lahtela-Kakkonen, M.; Moaddel, R. N-Acylethanolamines Bind to SIRT6. *ChemBioChem* **2016**, *17*, 77–81.
- (103) Rahnasto-Rilla, M.; Tyni, J.; Huovinen, M.; Jarho, E.; Kulikowicz, T.; Ravichandran, S.; Bohr, V. A.; Ferrucci, L.; Lahtela-Kakkonen, M.; Moaddel, R. Natural polyphenols as sirtuin 6 modulators. *Sci. Rep.* **2018**, *8*, 4163.
- (104) You, W.; Zheng, W.; Weiss, S.; Chua, K. F.; Steegborn, C. Structural basis for the activation and inhibition of Sirtuin 6 by quercetin and its derivatives. *Sci. Rep.* **2019**, *9*, 19176.
- (105) Tadera, K.; Minami, Y.; Takamatsu, K.; Matsuoka, T. Inhibition of α -Glucosidase and α -Amylase by Flavonoids. *J. Nutr. Sci. Vitaminol.* **2006**, *52*, 149–153.
- (106) Proenca, C.; Freitas, M.; Ribeiro, D.; Oliveira, E. F. T.; Sousa, J. L. C.; Tome, S. M.; Ramos, M. J.; Silva, A. M. S.; Fernandes, P. A.; Fernandes, E. α -Glucosidase inhibition by flavonoids: an in vitro and in silico structure-activity relationship study. *J. Enzyme Inhib. Med. Chem.* **2017**, *32*, 1216–1228.
- (107) Zhu, J.; Chen, C.; Zhang, B.; Huang, Q. The inhibitory effects of flavonoids on α -amylase and α -glucosidase. *Crit. Rev. Food Sci. Nutr.* **2020**, *60*, 695–708.
- (108) Boege, F.; Straub, T.; Kehr, A.; Boesenberg, C.; Christiansen, K.; Andersen, A.; Jakob, F.; Kohrle, J. Selected novel flavones inhibit the DNA binding or the DNA religation step of eukaryotic topoisomerase I. *J. Biol. Chem.* **1996**, *271*, 2262–2270.
- (109) Chowdhury, A. R.; Sharma, S.; Mandal, S.; Goswami, A.; Mukhopadhyay, S.; Majumder, H. K. Luteolin, an emerging anti-cancer flavonoid, poisons eukaryotic DNA topoisomerase I. *Biochem. J.* **2002**, *366*, 653–661.
- (110) Lopez-Lazaro, M.; Willmore, E.; Austin, C. A. The dietary flavonoids myricetin and fisetin act as dual inhibitors of DNA topoisomerases I and II in cells. *Mutat. Res., Genet. Toxicol. Environ. Mutagen.* **2010**, *696*, 41–47.
- (111) Cantero, G.; Campanella, C.; Mateos, S.; Cortes, F. Topoisomerase II inhibition and high yield of endoreduplication induced by the flavonoids luteolin and quercetin. *Mutagenesis* **2006**, *21*, 321–325.
- (112) Habermeyer, M.; Fritz, J.; Barthelmes, H. U.; Christensen, M. O.; Larsen, M. K.; Boege, F.; Marko, D. Anthocyanidins Modulate the Activity of Human DNA Topoisomerases I and II and Affect Cellular DNA Integrity. *Chem. Res. Toxicol.* **2005**, *18*, 1395–1404.
- (113) Lee, W. J.; Shim, J. Y.; Zhu, B. T. Mechanisms for the inhibition of DNA methyltransferases by tea catechins and bioflavonoids. *Mol. Pharmacol.* **2005**, *68*, 1018–1030.
- (114) Zwergel, C.; Valente, S.; Mai, A. DNA Methyltransferases Inhibitors from Natural Sources. *Curr. Top. Med. Chem.* **2015**, *16*, 680–696.
- (115) Priyadarsini, R. V.; Vinothini, G.; Murugan, R. S.; Manikandan, P.; Nagini, S. The flavonoid quercetin modulates the hallmark capabilities of hamster buccal pouch tumors. *Nutr. Cancer* **2011**, *63*, 218–226.
- (116) Xiao, X.; Shi, D.; Liu, L.; Wang, J.; Xie, X.; Kang, T.; Deng, W. Quercetin suppresses cyclooxygenase-2 expression and angiogenesis through inactivation of P300 signaling. *PLoS One* **2011**, *6*, No. e22934.
- (117) Lee, W. J.; Chen, Y. R.; Tseng, T. H. Quercetin induces FasL-related apoptosis, in part, through promotion of histone H3 acetylation in human leukemia HL-60 cells. *Oncol. Rep.* **2011**, *25*, 583–591.
- (118) Bisson, J.; McAlpine, J. B.; Friesen, J. B.; Chen, S. N.; Graham, J.; Pauli, G. F. Can Invalid Bioactives Undermine Natural Product-Based Drug Discovery? *J. Med. Chem.* **2016**, *59*, 1671–1690.
- (119) Baell, J. B. Feeling Nature's PAINS: Natural Products, Natural Product Drugs, and Pan Assay Interference Compounds (PAINS). *J. Nat. Prod.* **2016**, *79*, 616–628.
- (120) Bohm, H. J.; Flohr, A.; Stahl, M. Scaffold hopping. *Drug Discovery Today: Technol.* **2004**, *1*, 217–224.
- (121) Hoffmann, T.; Gastreich, M. The next level in chemical space navigation: going far beyond enumerable compound libraries. *Drug Discovery Today* **2019**, *24*, 1148–1156.
- (122) Paul, D.; Sanap, G.; Shenoy, S.; Kalyane, D.; Kalia, K.; Tekade, R. K. Artificial intelligence in drug discovery and development. *Drug Discovery Today* **2021**, *26*, 80–93.
- (123) Rahnasto-Rilla, M. K.; McLoughlin, P.; Kulikowicz, T.; Doyle, M.; Bohr, V. A.; Lahtela-Kakkonen, M.; Ferrucci, L.; Hayes, M.; Moaddel, R. The Identification of a SIRT6 Activator from Brown Algae *Fucus distichus*. *Mar. Drugs* **2017**, *15*, 190.
- (124) You, W.; Rotili, D.; Li, T. M.; Kambach, C.; Meleshin, M.; Schutkowski, M.; Chua, K. F.; Mai, A.; Steegborn, C. Structural Basis of Sirtuin 6 Activation by Synthetic Small Molecules. *Angew. Chem., Int. Ed.* **2017**, *56*, 1007–1011.
- (125) Iachettini, S.; Trisciuglio, D.; Rotili, D.; Lucidi, A.; Salvati, E.; Zizza, P.; Di Leo, L.; Del Bufalo, D.; Ciriolo, M. R.; Leonetti, C.; Steegborn, C.; Mai, A.; Rizzo, A.; Biroccio, A. Pharmacological activation of SIRT6 triggers lethal autophagy in human cancer cells. *Cell Death Dis.* **2018**, *9*, 996.
- (126) Kim, J. H.; Lee, J. M.; Kim, J. H.; Kim, K. R. Fluvastatin activates sirtuin 6 to regulate sterol regulatory element-binding proteins and AMP-activated protein kinase in HepG2 cells. *Biochem. Biophys. Res. Commun.* **2018**, *503*, 1415–1421.
- (127) You, W.; Steegborn, C. Structural Basis for Activation of Human Sirtuin 6 by Fluvastatin. *ACS Med. Chem. Lett.* **2020**, *11*, 2285–2289.
- (128) Huang, Z.; Zhao, J.; Deng, W.; Chen, Y.; Shang, J.; Song, K.; Zhang, L.; Wang, C.; Lu, S.; Yang, X.; He, B.; Min, J.; Hu, H.; Tan, M.;

- Xu, J.; Zhang, Q.; Zhong, J.; Sun, X.; Mao, Z.; Lin, H.; Xiao, M.; Chin, Y. E.; Jiang, H.; Xu, Y.; Chen, G.; Zhang, J. Identification of a cellularly active SIRT6 allosteric activator. *Nat. Chem. Biol.* **2018**, *14*, 1118–1126.
- (129) Shang, J. L.; Ning, S. B.; Chen, Y. Y.; Chen, T. X.; Zhang, J. MDL-800, an allosteric activator of SIRT6, suppresses proliferation and enhances EGFR-TKIs therapy in non-small cell lung cancer. *Acta Pharmacol. Sin.* **2021**, *42*, 120–131.
- (130) You, W.; Steegborn, C. Binding site for activator MDL-801 on SIRT6. *Nat. Chem. Biol.* **2021**, *17*, 519.
- (131) Huang, Z.; Zhao, J.; Deng, W.; Chen, Y.; Shang, J.; Song, K.; Zhang, L.; Wang, C.; Lu, S.; Yang, X.; He, B.; Min, J.; Hu, H.; Tan, M.; Xu, J.; Zhang, Q.; Zhong, J.; Sun, X.; Mao, Z.; Lin, H.; Xiao, M.; Chin, Y. E.; Jiang, H.; Shen, H.; Xu, Y.; Chen, G.; Zhang, J. Reply to: Binding site for MDL-801 on SIRT6. *Nat. Chem. Biol.* **2021**, *17*, 522–523.
- (132) Shang, J.; Zhu, Z.; Chen, Y.; Song, J.; Huang, Y.; Song, K.; Zhong, J.; Xu, X.; Wei, J.; Wang, C.; Cui, L.; Liu, C. Y.; Zhang, J. Small-molecule activating SIRT6 elicits therapeutic effects and synergistically promotes anti-tumor activity of vitamin D₃ in colorectal cancer. *Theranostics* **2020**, *10*, 5845–5864.
- (133) Hobaus, J.; Hummel, D. M.; Thiem, U.; Fetahu, I. S.; Aggarwal, A.; Mullauer, L.; Heller, G.; Egger, G.; Mesteri, I.; Baumgartner-Parzer, S.; Kallay, E. Increased copy-number and not DNA hypomethylation causes overexpression of the candidate proto-oncogene CYP24A1 in colorectal cancer. *Int. J. Cancer* **2013**, *133*, 1380–1388.
- (134) Sun, H.; Wang, C.; Hao, M.; Sun, R.; Wang, Y.; Liu, T.; Cong, X.; Liu, Y. CYP24A1 is a potential biomarker for the progression and prognosis of human colorectal cancer. *Hum. Pathol.* **2016**, *50*, 101–108.
- (135) Pereira, F.; Larriba, M. J.; Muñoz, A. Vitamin D and colon cancer. *Endocr.-Relat. Cancer* **2012**, *19*, R51–R71.
- (136) Ng, K.; Nimeiri, H. S.; McCleary, N. J.; Abrams, T. A.; Yurgelun, M. B.; Cleary, J. M.; Rubinson, D. A.; Schrag, D.; Miksad, R.; Bullock, A. J.; Allen, J.; Zuckerman, D.; Chan, E.; Chan, J. A.; Wolpin, B. M.; Constantine, M.; Weckstein, D. J.; Faggen, M. A.; Thomas, C. A.; Kournioti, C.; Yuan, C.; Ganser, C.; Wilkinson, B.; Mackintosh, C.; Zheng, H.; Hollis, B. W.; Meyerhardt, J. A.; Fuchs, C. S. Effect of High-Dose vs Standard-Dose Vitamin D₃ Supplementation on Progression-Free Survival Among Patients With Advanced or Metastatic Colorectal Cancer: The SUNSHINE Randomized Clinical Trial. *JAMA* **2019**, *321*, 1370–1379.
- (137) Carraway, H. E.; Malkaram, S. A.; Cen, Y.; Shatnawi, A.; Fan, J.; Ali, H. E. A.; Abd Elmageed, Z. Y.; Buttolph, T.; Denvir, J.; Primerano, D. A.; Fandy, T. E. Activation of SIRT6 by DNA hypomethylating agents and clinical consequences on combination therapy in leukemia. *Sci. Rep.* **2020**, *10*, 10325.
- (138) Chen, X.; Sun, W.; Huang, S.; Zhang, H.; Lin, G.; Li, H.; Qiao, J.; Li, L.; Yang, S. Discovery of Potent Small-Molecule SIRT6 Activators: Structure-Activity Relationship and Anti-Pancreatic Ductal Adenocarcinoma Activity. *J. Med. Chem.* **2020**, *63*, 10474–10495.
- (139) Jafari, R.; Almqvist, H.; Axelsson, H.; Ignatshchenko, M.; Lundback, T.; Nordlund, P.; Martinez Molina, D. The cellular thermal shift assay for evaluating drug target interactions in cells. *Nat. Protoc.* **2014**, *9*, 2100–2122.
- (140) Savitski, M. M.; Reinhard, F. B.; Franken, H.; Werner, T.; Savitski, M. F.; Eberhard, D.; Molina, D. M.; Jafari, R.; Dovega, R. B.; Klaeger, S.; Kuster, B.; Nordlund, P.; Bantscheff, M.; Drewes, G. Tracking cancer drugs in living cells by thermal profiling of the proteome. *Science* **2014**, *346*, 1255784.
- (141) Franken, H.; Mathieson, T.; Childs, D.; Sweetman, G. M.; Werner, T.; Togel, I.; Doce, C.; Gade, S.; Bantscheff, M.; Drewes, G.; Reinhard, F. B.; Huber, W.; Savitski, M. M. Thermal proteome profiling for unbiased identification of direct and indirect drug targets using multiplexed quantitative mass spectrometry. *Nat. Protoc.* **2015**, *10*, 1567–93.
- (142) Hau, M.; Zenk, F.; Ganesan, A.; Iovino, N.; Jung, M. Cellular analysis of the action of epigenetic drugs and probes. *Epigenetics* **2017**, *12*, 308–322.
- (143) Simon, G. M.; Niphakis, M. J.; Cravatt, B. F. Determining target engagement in living systems. *Nat. Chem. Biol.* **2013**, *9*, 200–205.
- (144) Huang, Y.; Furuno, M.; Arakawa, T.; Takizawa, S.; de Hoon, M.; Suzuki, H.; Arner, E. A framework for identification of on- and off-target transcriptional responses to drug treatment. *Sci. Rep.* **2019**, *9*, 17603.
- (145) Sacca, R.; Engle, S. J.; Qin, W.; Stock, J. L.; McNeish, J. D. Genetically Engineered Mouse Models in Drug Discovery Research. *Methods Mol. Biol.* **2010**, *602*, 37–54.
- (146) Bitterman, K. J.; Anderson, R. M.; Cohen, H. Y.; Latorre-Esteves, M.; Sinclair, D. A. Inhibition of silencing and accelerated aging by nicotinamide, a putative negative regulator of yeast Sir2 and human SIRT1. *J. Biol. Chem.* **2002**, *277*, 45099–45107.
- (147) Jackson, M. D.; Schmidt, M. T.; Oppenheimer, N. J.; Denu, J. M. Mechanism of nicotinamide inhibition and transglycosidation by Sir2 histone/protein deacetylases. *J. Biol. Chem.* **2003**, *278*, 50985–50998.
- (148) Avalos, J. L.; Bever, K. M.; Wolberger, C. Mechanism of sirtuin inhibition by nicotinamide: Altering the NAD(+) cosubstrate specificity of a Sir2 enzyme. *Mol. Cell* **2005**, *17*, 855–868.
- (149) Hu, J.; He, B.; Bhargava, S.; Lin, H. A fluorogenic assay for screening Sirt6 modulators. *Org. Biomol. Chem.* **2013**, *11*, 5213–5216.
- (150) Bolivar, B. E.; Welch, J. T. Studies of the Binding of Modest Modulators of the Human Enzyme, Sirtuin 6, by STD NMR. *ChemBioChem* **2017**, *18*, 931–940.
- (151) Madsen, A. S.; Andersen, C.; Daoud, M.; Anderson, K. A.; Laursen, J. S.; Chakladar, S.; Huynh, F. K.; Colaco, A. R.; Backos, D. S.; Fristrup, P.; Hirsche, M. D.; Olsen, C. A. Investigating the Sensitivity of NAD(+)-dependent Sirtuin Deacylation Activities to NADH. *J. Biol. Chem.* **2016**, *291*, 7128–7141.
- (152) Fatkins, D. G.; Monnot, A. D.; Zheng, W. N-epsilon-thioacetyllysine: A multi-facet functional probe for enzymatic protein lysine N-epsilon-deacetylation. *Bioorg. Med. Chem. Lett.* **2006**, *16*, 3651–3656.
- (153) Kokkonen, P.; Rahnasto-Rilla, M.; Kiviranta, P. H.; Huhtiniemi, T.; Laitinen, T.; Poso, A.; Jarho, E.; Lahtela-Kakkonen, M. Peptides and Pseudopeptides as SIRT6 Deacetylation Inhibitors. *ACS Med. Chem. Lett.* **2012**, *3*, 969–974.
- (154) He, B.; Hu, J.; Zhang, X.; Lin, H. Thiomyristoyl peptides as cell-permeable Sirt6 inhibitors. *Org. Biomol. Chem.* **2014**, *12*, 7498–7502.
- (155) Liu, J.; Zheng, W. Cyclic peptide-based potent human SIRT6 inhibitors. *Org. Biomol. Chem.* **2016**, *14*, 5928–5935.
- (156) Sociali, G.; Liessi, N.; Grozio, A.; Caffa, I.; Parenti, M. D.; Ravera, S.; Tasso, B.; Benzi, A.; Nencioni, A.; Del Rio, A.; Robina, I.; Millo, E.; Bruzzone, S. Differential modulation of SIRT6 deacetylase and deacylase activities by lysine-based small molecules. *Mol. Diversity* **2020**, *24*, 655–671.
- (157) Kamiyama, O.; Sanae, F.; Ikeda, K.; Higashi, Y.; Minami, Y.; Asano, N.; Adachi, I.; Kato, A. In vitro inhibition of α -glucosidases and glycogen phosphorylase by catechin gallates in green tea. *Food Chem.* **2010**, *122*, 1061–1066.
- (158) Berger, S. J.; Gupta, S.; Belfi, C. A.; Gosky, D. M.; Mukhtar, H. Green tea constituent (–)-epigallocatechin-3-gallate inhibits topoisomerase I activity in human colon carcinoma cells. *Biochem. Biophys. Res. Commun.* **2001**, *288*, 101–105.
- (159) Bandele, O. J.; Osheroff, N. (–)-Epigallocatechin Gallate, A Major Constituent of Green Tea, Poisons Human Type II Topoisomerases. *Chem. Res. Toxicol.* **2008**, *21*, 936–943.
- (160) Tao, L.; Park, J. Y.; Lambert, J. D. Differential prooxidative effects of the green tea polyphenol, (–)-epigallocatechin-3-gallate, in normal and oral cancer cells are related to differences in sirtuin 3 signaling. *Mol. Nutr. Food Res.* **2015**, *59*, 203–211.
- (161) Wood, M.; Rymarchyk, S.; Zheng, S.; Cen, Y. Trichostatin A inhibits deacetylation of histone H3 and p53 by SIRT6. *Arch. Biochem. Biophys.* **2018**, *638*, 8–17.
- (162) You, W.; Steegborn, C. Structural Basis of Sirtuin 6 Inhibition by the Hydroxamate Trichostatin A: Implications for Protein Deacylase Drug Development. *J. Med. Chem.* **2018**, *61*, 10922–10928.
- (163) Parenti, M. D.; Grozio, A.; Bauer, I.; Galeno, L.; Damonte, P.; Millo, E.; Sociali, G.; Franceschi, C.; Ballestrero, A.; Bruzzone, S.; Del Rio, A.; Nencioni, A. Discovery of Novel and Selective SIRT6 Inhibitors. *J. Med. Chem.* **2014**, *57*, 4796–4804.

(164) Sociali, G.; Magnone, M.; Ravera, S.; Damonte, P.; Vigliarolo, T.; von Holtey, M.; Vellone, V. G.; Millo, E.; Caffa, I.; Cea, M.; Parenti, M. D.; Del Rio, A.; Murone, M.; Mostoslavsky, R.; Grozio, A.; Nencioni, A.; Bruzzone, S. Pharmacological Sirt6 inhibition improves glucose tolerance in a type 2 diabetes mouse model. *FASEB J.* **2017**, *31*, 3138–3149.

(165) Cea, M.; Cagnetta, A.; Adamia, S.; Acharya, C.; Tai, Y.-T.; Fulciniti, M.; Ohguchi, H.; Munshi, A.; Acharya, P.; Bhasin, M. K.; Zhong, L.; Carrasco, R.; Monacelli, F.; Ballestrero, A.; Richardson, P.; Gobbi, M.; Lemoli, R. M.; Munshi, N.; Hideshima, T.; Nencioni, A.; Chauhan, D.; Anderson, K. C. Evidence for a role of the histone deacetylase SIRT6 in DNA damage response of multiple myeloma cells. *Blood* **2016**, *127*, 1138–1150.

(166) Sociali, G.; Galeno, L.; Parenti, M. D.; Grozio, A.; Bauer, I.; Passalacqua, M.; Boero, S.; Donadini, A.; Millo, E.; Bellotti, M.; Sturla, L.; Damonte, P.; Puddu, A.; Ferroni, C.; Varchi, G.; Franceschi, C.; Ballestrero, A.; Poggi, A.; Bruzzone, S.; Nencioni, A.; Del Rio, A. Quinazolinone SIRT6 inhibitors sensitize cancer cells to chemotherapeutics. *Eur. J. Med. Chem.* **2015**, *102*, 530–539.

(167) Liu, Y.; Xie, Q. R.; Wang, B.; Shao, J.; Zhang, T.; Liu, T.; Huang, G.; Xia, W. Inhibition of SIRT6 in prostate cancer reduces cell viability and increases sensitivity to chemotherapeutics. *Protein Cell* **2013**, *4*, 702–710.

(168) Damonte, P.; Sociali, G.; Parenti, M. D.; Soncini, D.; Bauer, I.; Boero, S.; Grozio, A.; von Holtey, M.; Piacente, F.; Becherini, P.; Sanguineti, R.; Salis, A.; Damonte, G.; Cea, M.; Murone, M.; Poggi, A.; Nencioni, A.; Del Rio, A.; Bruzzone, S. SIRT6 inhibitors with salicylate-like structure show immunosuppressive and chemosensitizing effects. *Bioorg. Med. Chem.* **2017**, *25*, 5849–5858.

(169) Yuen, L. H.; Dana, S.; Liu, Y.; Bloom, S. I.; Thorsell, A. G.; Neri, D.; Donato, A. J.; Kireev, D.; Schuler, H.; Franzini, R. M. A Focused DNA-Encoded Chemical Library for the Discovery of Inhibitors of NAD(+)-Dependent Enzymes. *J. Am. Chem. Soc.* **2019**, *141*, 5169–5181.

(170) Cardus, A.; Uryga, A. K.; Walters, G.; Erusalimsky, J. D. SIRT6 protects human endothelial cells from DNA damage, telomere dysfunction, and senescence. *Cardiovasc. Res.* **2013**, *97*, 571–579.

(171) Sun, W.; Chen, X.; Huang, S.; Li, W.; Tian, C.; Yang, S.; Li, L. Discovery of 5-(4-methylpiperazin-1-yl)-2-nitroaniline derivatives as a new class of SIRT6 inhibitors. *Bioorg. Med. Chem. Lett.* **2020**, *30*, 127215.

(172) Shi, B.; Zhou, Y.; Huang, Y.; Zhang, J.; Li, X. Recent advances on the encoding and selection methods of DNA-encoded chemical library. *Bioorg. Med. Chem. Lett.* **2017**, *27*, 361–369.

(173) Franzini, R. M.; Randolph, C. Chemical Space of DNA-Encoded Libraries. *J. Med. Chem.* **2016**, *59*, 6629–6644.

(174) Renaud, J. P.; Chung, C. W.; Danielson, U. H.; Egner, U.; Hennig, M.; Hubbard, R. E.; Nar, H. Biophysics in drug discovery: impact, challenges and opportunities. *Nat. Rev. Drug Discovery* **2016**, *15*, 679–98.

(175) Fiorentino, F.; Sauer, J. B.; Qiu, X.; Corey, R. A.; Cassidy, C. K.; Mynors-Wallis, B.; Mehmood, S.; Bolla, J. R.; Stansfeld, P. J.; Robinson, C. V. Dynamics of an LPS translocon induced by substrate and an antimicrobial peptide. *Nat. Chem. Biol.* **2021**, *17*, 187–195.

(176) McDowell, M. A.; Heimes, M.; Fiorentino, F.; Mehmood, S.; Farkas, A.; Coy-Vergara, J.; Wu, D.; Bolla, J. R.; Schmid, V.; Heinze, R.; Wild, K.; Flemming, D.; Pfeffer, S.; Schwappach, B.; Robinson, C. V.; Sinning, I. Structural Basis of Tail-Anchored Membrane Protein Biogenesis by the GET Insertase Complex. *Mol. Cell* **2020**, *80*, 72–86.e7.

(177) Bolla, J. R.; Howes, A. C.; Fiorentino, F.; Robinson, C. V. Assembly and regulation of the chlorhexidine-specific efflux pump AceI. *Proc. Natl. Acad. Sci. U. S. A.* **2020**, *117*, 17011–17018.